Dynamical and Statistical Properties of Lorentz Lattice Gases

A Thesis
Presented to
The Academic Faculty

by

Milena Khlabystova

In Partial Fulfillment
of the Requirements for the Degree
Doctor of Philosophy

School of Mathematics
Georgia Institute of Technology
April 2003

Dynamical and Statistical Properties of Lorentz Lattice Gases

Approved by:

Leonid Bunimovich, Committee Chair	Mihai Ciucu
Thomas Morley	Federico Bonetto
Dana Randall	

Date Approved _____

ACKNOWLEDGEMENTS

I would like to express my appreciation to the Georgia Institute of Technology for providing such a stimulating learning environment, as well as the financial support that has made this study possible.

I am grateful to the School of Mathematics which has tremendously contributed to my education through lectures, academic discussions, and teaching opportunities; and to my Oral Examination Committee - Professors R. Lyons, J. Steif and T. Morley - for their insightful criticism of my early work. I would also like to thank Professor L. de Haan of the Erasmus University Rotterdam and Dr. L. Peng for their valuable suggestions about possible approaches to statistical analysis of the simulation data. And, the members of my Reading Committee - Professors D. Randall, F. Bonetto, M. Ciucu and T. Morley - for being so generous with their time and efforts on behalf of this work.

My special thanks to my mentors, Professors L. Dmitrieva and Yu. Kuperin of the St. Petersburg State University for giving me the inspiration and fostering my love of mathematics.

Of course, this work would not have been possible without the continual encouragement, direction, and support of my research advisor, Professor L. Bunimovich. I would like to thank him for giving me the opportunity to participate in research projects and co-authored publications. It has been a great honor and a great pleasure to work under his supervision.

I would also like to thank Professor C. Jacobson, Ms. J. Smythe, and the staff of the School of Mathematics for all their assistance and support. On this note, I would like to extend my heartfelt thanks to Ms. Debbie Harper from the Office of International Education for her endless patience and continual assistance.

Finally, I thank my friends Beth, Victor, Jose-Miguel and Claudia for supporting my work and making this a fun experience, Billy and Buddy for their warmth and comfort, and, of course, Cath for all of the above and proofreading my work.

TABLE OF CONTENTS

LIST OF TABLES

LIST OF FIGURES

LIST OF SYMBOLS OR ABBREVIATIONS

BS	Back-scatterer.
FLLG	Flipping Lorentz lattice gas(es).
FM	Flipping mirror (model).
FR	Flipping rotator (model).
FS	Forward scatterer.
LLG	Lorentz lattice gas(es).
LR	Left rotator.
LS	Left scatterer.
NOS	Non-oriented scatterers.
OS	Oriented scatterers.
PRL	Poisson random lattice.
RLLG	Rotating Lorentz lattice gas(es).
RR	Right rotator.
RS	Right scatterer.
SLLG	Static Lorentz lattice gas(es).
SM	Static mirror (model).
SR	Static rotator (model).
VRL	Vectorizable random lattice.
WRE	Walk(s) in rigid environments.

SUMMARY

This thesis studies the motion of a single particle, or an ensemble of particles, in Lorentz lattice gas (LLG) models with flipping scatterers (FLLG) and with rotating scatterers (RLLG). In the first, a particle moves between the vertices of a lattice with unit speed, where the choice of next vertex on its path is determined by the type of scatterer at the current vertex. Initially, the scatterers of two types are randomly distributed among the vertices of the lattice; they change their type (flip) every time they are hit by a particle. It is well known that in LLG with flipping rotators on the regular triangular lattice, the particle ultimately propagates in one direction in a strip. It appears that this result can be extended to LLG with flipping rotators on Delaunay random lattices, but that it is not true for the FLLG on the square or hexagonal lattices. The study of particle interactions on the triangular lattice presented in this text shows that two propagating particles may change their propagation strips, after colliding with each other.

The FLLG model on the Delaunay lattice exhibits a peculiar behaviour by which the trajectory of a particle, while being confined to a strip, may be bounded. This demonstrates that the randomness of the lattice can cause the localization of orbits. Another result shows that, for a certain general class of random lattices, the orbit of a particle is bounded with probability one.

In the Lorentz gas model with rotating scatterers, infinitely many particles move in an environment of freely rotating disks whose centers are fixed on a regular triangular lattice. Collisions of the particles with the disks are assumed to be elastic. The simplest orbits of this system are found by considering its one-dimensional one-particle reduction. The model has only one parameter which can be viewed as the amount

of energy transfer between scatterers and particles in a collision. Exact solutions of the reduced system are found for several values of this parameter. For some of these values, the dynamics is shown to be, in many respects, similar to the dynamics of the deterministic Lorentz lattice gases.

The only parameter of the model is the amount of energy transfer between the particle and the disk during their collision. Exact solutions of the one-dimensionalred one-particle reduction of this system are obtained for several values of this parameter. These solutions also represent the simplest orbits of the original system. In some cases, the dynamics is shown to be in many respects similar to the dynamics of the deterministic Lorentz lattice gases.

A new class of LLG models, which includes the FLLG model as one of its extreme cases, was recently introduced. In these models, the particle still moves with the unit speed in a random array of scatterers, but now the type of scatterer at a vertex changes after the r-th visit of the particle to this vertex, where $1 \leq r \leq \infty$. Such deterministic cellular automata are referred to as walks in rigid environments (WRE). They form the simplest dynamical models with sub-diffusive, diffusive and super-diffusive behaviour. Continuous limits of kinetic equations are obtained for one-dimensional models of this class. Due to the deterministic character of the dynamics, these continuous limit equations are of the Euler type rather than the diffusive type. The reason is that fluctuations in these models are relatively small and there is no scaling of probabilities similar, for example, to that in the case of biased random walk that can account for them.

Finally, the results of numerical simulations of one-dimensional multi-particle LLG with flipping scatterers are presented. The particles are distributed with some uniform density over the lattice vertices, and the multi-particle collisions proceed according to some specified rule. The statistical properties of two variations of the FLLG

model with different rules are studied. For both rules the distribution of particle displacements appears to be Gaussian at any time, and the mean square particle displacement grows linearly with time, thereby exhibiting diffusive behaviour.

CHAPTER I

INTRODUCTION

We consider a class of dynamical systems that model the motion of an object (electron, ant, ray of light, Turing read/write head) on a simple undirected infinite graph G. At each time step the object hops from a vertex to one of its neighboring vertices along the graph's edges. Knowing the edge via which it arrived at the current vertex $g \in G$, the choice of next vertex on its path is completely determined by the type of deterministic scattering rule at g. A scattering rule, or a scatterer, is defined as a map $s_g : \ A_{in}(g) \to A_{out}(g)$ from the set of all incoming edges of g to the set of all edges which originate at g. (Note that, since G is undirected, these sets can be identified.) Thus, if a particle arrives at g via some edge e, it will leave the vertex via $s_g(e)$. We denote the set of all possible scatterers on G as S. If G is a regular graph of degree d, then $card\ S = d^d$. We assume in this text that the scatterers are initially placed at the vertices of G independently, unless otherwise specified.

Systems of this type are referred to as Lorentz lattice gases (LLG). They have attracted significant interest in recent years because of the rich dynamics that they exhibit on the large scale, while being relatively simple on the microscopic level. This is a consequence of the fact that LLG are neither purely stochastic nor purely deterministic models. Instead, both types of behaviour contribute to the dynamics (evolution) of the system. Aside from being of purely mathematical interest, these models have found their way into a wide range of other fields: biochemistry and artificial life [47], computational fluid dynamics [1], [56], graph theory [37], [36] and theoretical computer science [27], [47], [6], to name a few. Potential applications

include studying the growth of the order-disorder or solid-liquid interface [51], simulating biomolecular functions or studying the dynamics of aggregate systems such as insect colonies [47]. Much of the activity in the field of hydrodynamics was motivated by the introduction of a perfectly isotropic lattice gas version of the Navier-Stokes equation by Frisch et.al. in [35] and simultaneously by Wolfram in [64]. Their model and its derivatives remain an effective simulation method for certain complex fluids such as microemulsions (see e.g. [3], [2] and references therein). Some LLG models have been shown to simulate the dynamics of a Turing machine and, therefore, are capable of universal computation [37]. An interesting model of parallel computation based on LLG has been proposed in [27]. Finally, we would like to mention that LLG could be useful for numerical simulations of partial differential equations. It has been shown that, given a little information about the structure of orbits in a 2D Turing machine, it may be possible to solve the inverse problem, i.e. recover the model from an observed orbit ([8], [20]).

In the classical Lorentz gas a particle moves in the Euclidean space $\mathbb{R}^3$ colliding elastically with randomly placed spheres. Introduced in [48] in connection with the study of electrical conductivity in metals, it serves as a model for the dynamics of an electron in a crystal. A simplified version of this model was developed by P. Ehrenfest and has become known as Ehrenfest's *wind-tree* model [30]. In this version the moving particle (wind) is elastically scattered by randomly placed diamonds (trees) whose diagonals are parallel to the coordinate axes. These two models are considered to be the simplest models for studying the diffusion of a particle in a random environment. However, the rigorous analysis of these models turned out to be quite complicated. In fact, the time-irreversible macroscopic dynamics (diffusion) in Lorentz gas has been rigorously derived from the time-reversible microscopic dynamics only in the case when the configuration of scatterers is periodic and under the condition that the free path of the particle is bounded (see [16], [17], [21]).

The difficulty associated with the study of the classical Lorentz gas naturally led to the development of simpler models. The Lorentz lattice gas cellular automata form one class of such simplified models. They can be thought of as a restriction of either of the classical models to some lattice in the Euclidean space, where a particle moves in an array of randomly distributed scatterers. In its most general form the LLG model was introduced in [8], allowing arbitrary time evolution of the scatterers at any lattice vertex.

The class of LLG models can be further divided into subclasses. Two such general subclasses have been of particular interest to researchers: LLG with *fixed scatterers*, a.k.a. static LLG (SLLG), where the environment of scatterers does not change in the course of evolution; and LLG with *flipping scatterers* (FLLG) which allow for the particle's feedback on the environment. In the latter case, the scattering rule at a lattice vertex changes every time this vertex is visited by a particle. Both SLLG and FLLG describe the deterministic motion of a particle in an environment of randomly distributed scatterers. Hence, the notion of *deterministic walks in random environments* seems appropriate. Other LLG subclasses include models with various degrees of randomness appearing in the scattering rules (see e.g. [18], [31]) as well as hybrid models ([40]).

The early LLG models include the static mirror (SM, [58]) and static rotator (SR, [42]) models on $\mathbb{Z}^2$. The former appears to be closely related to bond percolation [39] and the problem of random tiling of the plane with Truchet tiles, also known as hull percolation [29], [54], [55], [57], [59]. Its relation to the formation of polymers and smart kinetic walks has also been noticed by various authors (see e.g. [7], [49], [65] and references therein). The flipping analogues of the mirror and rotator models, FM and FR, were introduced in [58] and [18] respectively, although similar models emerged independently in several other fields. Among those are the *industrious ant* model in biochemistry [47] and the *turmites* model in theoretical computer science

[27]. The notion of static and flipping Lorentz lattice gases have been subsequently extended to the other lattices as well. The LLG models on a triangular lattice were introduced in [18] and [44], on hexagonal and quasi- lattices in [62], and on Delaunay random lattices in [63].

The majority of the rigorous mathematical results concerning LLG models deal with the problem of the existence of unbounded orbits, while the numerical results typically explore their diffusive properties. Physics literature is particularly interested in the asymptotic distribution of the position and velocity of the particle. Note, however, that there is no "common" approach to studying these systems, that would work for a whole class of models. Rather, each model requires a separate consideration.

Bunimovich and Troubetzkoy studied both the static and flipping LLG on regular square and triangular lattices, and proved a number of theorems about the boundedness of orbits in those models [18] and their topological properties [19]. They also showed that in some cases it is possible to solve the inverse problem, i.e. determine the configuration of scatterers on the lattice from the topology of the particle trajectories [20]. Table 1 lists the available results for the static and flipping Lorentz lattice gases on these lattices as per [18], [41], [58], [45], [65]. Note from the table that it is still unclear whether there are unbounded trajectories in the non-fully occupied models. The simulations performed by E.G.D.Cohen et.al., however, suggest that all orbits eventually close [24]. In this text, we study FLLG on one- and two-dimensional lattices, both regular and random (some results on higher dimensional models have been obtained in [8], [9]).

The diffusion behaviour in LLG with a variety of scattering rules has been studied numerically by E.G.D. Cohen in collaboration with T. W. Ruijgrok ([58]), X. P. Kong ([44], [46], [65], [45]) and F. Wang ([26], [24], [62], [61], [63]). A good review of their findings can be found in [25]. The results of their simulations suggest that LLG on regular lattices may experience several types of diffusion depending on the

Table 1: The existence of periodic and unbounded trajectories in single-particle LLG models on the regular square ($\mathbb{Z}^2$) and triangular ($\mathbb{T}^2$) lattices (see references in the text). Footnotes denote the conditional statements, i.e. the results which hold only if the corresponding condition is satisfied: [1] $C_L > 0$ & $C_R > 0$, [2] $C_L \geq p_c \mid C_R \geq p_c$, [3] $C_L = 0 \mid C_R = 0$. Here C_L and C_R are the (initial) concentrations of left and right scatterers in the corresponding model and p_c is the critical parameter for site percolation on the corresponding lattice ($p_c = 1/2$ for $\mathbb{T}^2$ and $p_c = 0.593$ for $\mathbb{Z}^2$). FO stands for "fully occupied" lattice ($C \equiv C_R + C_L = 1$), and NFO stands for "not fully occupied" lattice ($C < 1$). All these results hold with probability 1 with respect to the probability measure on the space of initial configurations of scatterers with fixed C_L and C_R.

Trajectories	Mirrors ($\mathbb{Z}^2$)		Rotators ($\mathbb{Z}^2$)		Mirrors ($\mathbb{T}^2$)		Rotators ($\mathbb{T}^2$)	
Static Models								
	FO	NFO	FO	NFO	FO	NFO	FO	NFO
periodic	yes[1]	yes	yes	yes[2]	yes	yes[2]	yes	yes[2]
unbounded	yes[3]	?	no	?	no	?	no	?
Flipping Models								
	FO	NFO	FO	NFO	FO	NFO	FO	NFO
periodic	no	no	no	yes	no	yes	no	yes
unbounded	yes	yes	yes	no	yes	no	yes	no

concentration of left and right scatterers on the lattice. Namely, for most values of the concentrations and most static scattering rules, the diffusion behaviour can be characterized as *anomalous* diffusion, where the mean square displacement of the particle grows linearly with time, but the distribution function of its position does not appear to be Gaussian. For certain critical values, which are lattice-dependent, *no diffusion* was observed as all particles got trapped in closed orbits in finite time. This behaviour is consistent with the above mentioned results by Bunimovich and Troubetzkoy. In addition, super-diffusion has been observed in the non-fully occupied SM model on $\mathbb{Z}^2$ for all concentrations of scatterers. The normal diffusive behaviour, however, was observed in the flipping models. This should be contrasted with the LLG models with purely probabilistic scattering rules where the diffusion is always normal (see e.g. [32], [31], [60]). These results are summarized in Table 2.

Mathematically these models belong to the class of *deterministic* cellular automata (CA) and describe the deterministic motion of particles in random media. Although, at first sight, they look somewhat similar to random walks, their properties are quite different. For instance, an orbit of a random walk which visits only a finite number of sites does not have to be periodic. On the contrary, a trajectory of an LLG model which visits only a finite number of vertices is always periodic [13]. The earlier discussion of the diffusion behaviour in the two models further illustrates this dissimilarity. Often, however, the properties of LLG models are quite counterintuitive. The recently proven ultimate propagation of a particle in a strip on the regular triangular lattice with flipping scatterers [41] is just one example of such unexpected behaviour.

All of the above models involve the motion of a single particle. But the models with many particles can be considered as well. In multi-particle LLG models it is usually assumed that the particles are distributed with uniform density over the lattice vertices, and that the particles do not interact with each other. It is interesting to note that, in the SLLG with many particles, the particle's dynamics is not affected by

Table 2: Diffusion behaviour in the square ($\mathbb{Z}^2$), triangular ($\mathbb{T}^2$), hexagonal ($\mathbb{H}^2$) and random ($\mathbb{D}^2$) Lorentz lattice gases observed in numerical simulations by Cohen et.al. (see references in the text). Here *no diffusion* means that the particle always gets trapped; *anomalous* diffusion means that the diffusion coefficient approaches a constant as $t \to \infty$, but neither the distribution function of the particle's position nor the kurtosis correspond to those of Gaussian distribution; *quasi-normal* diffusion is similar to the anomalous diffusion except that the kurtosis does correspond to that of normal distribution; and *super*-diffusion means that the mean square particle displacement grows faster than t. As before, C_L and C_R denote the concentrations of left and right scatterers, and $C = C_L + C_R$.

Lattice	Model	Condition	Diffusion Behaviour
Static Models			
$\mathbb{Z}^2$	SM	$C = 1$	anomalous
		$C < 1$	super
	SR		no diffusion except on two symmetric curves in (C_L, C_R) plane where the diffusion is anomalous
$\mathbb{T}^2$	SM, SR	$C_L = C_R$	anomalous
		$C_L \neq C_R$	no diffusion
$\mathbb{H}^2$	SM	$C = 1$	no diffusion
	SR	$C = 1$	no diffusion except at two symmetric critical points where the diffusion is anomalous
$\mathbb{D}^2$	SR	$C = 1$ & $C_L \neq C_R$	no diffusion
		$C = 1$ & $C_L = C_R$	anomalous
Flipping Models			
$\mathbb{Z}^2$	FM		normal
	FR	$C = 1$	normal
		$C < 1$	no diffusion
$\mathbb{T}^2$	FM, FR	$C = 1$	propagation
	FM, FR	$C < 1$	quasi-normal
$\mathbb{H}^2$	FM, FR	$C = 1$	no diffusion
$\mathbb{D}^2$	FR	$C = 1$	quasi-normal (PRL) or normal (VRL)

the presence of other particles and can, therefore, be completely described by studying the one-particle model alone. On the contrary, since the particles constantly change the environment in which other particles move, multi-particle flipping LLG present a rather complex system in which the particles interact with each other indirectly. For example, a collision of two propagating particles in the FR model can result in their scattering off one another, or it can lead to new joint collective motion, and possibly, a joint periodic orbit. A subsequent collision with the third particle may break the association, and result in the three propagating particles again (see e.g. [51] and references therein). Such systems however, are highly non-trivial, and to the best of our knowledge, there are no rigorous results concerning their dynamics, with the exception of some topological results obtained by Bunimovich and Troubetzkoy in [18]. In this text we perform statistical analysis of one such multi-particle system, namely, the one-dimensional LLG with flipping scatterers.

Recently, a new class of LLG models called *walks in rigid environment* (WRE) was introduced in [10]. This class includes both LLG with fixed and flipping scatterers as the extreme cases. According to this paper, an environment is said to have rigidity r if the type of scatterer at a lattice vertex changes after the r-th visit of a particle to this vertex. Thus, the LLG with flipping scatterers can be viewed as WRE with rigidity one, and LLG with fixed scatterers as WRE with infinite rigidity. It has been shown that models which belong to this class are exactly solvable in dimension one. In addition, the LLG model with flipping rotators on a regular triangular lattice has been solved for the motion of one particle [41]. It was shown that the particle always builds a glider, similar to the one in Conway's Game of Life, which moves with random velocity. The average velocity of the glider depends on the states of scatterers placed at the lattice vertices. We study the interactions of such propagating particles and demonstrate that, when particles collide (interact), the corresponding gliders may change their directions of propagation.

It was shown in [28] that the classical Lorentz gas does not satisfy the local thermal equilibrium condition because, in this model, the scatterers are inert and, therefore, do not participate in the energy exchange. To overcome this deficiency, a modification of the periodic Lorentz gas was introduced in [50]. In this modification, referred to in this text as LLG with rotating scatterers (RLLG), the lattice vertices are occupied by freely rotating disks with fixed centers. Non-interacting particles are moving in an array of such disks and get scattered by them according to the rules of perfectly elastic collisions. It has essentially only one parameter which describes the amount of energy transfer between a particle and a disk during their collision. We find exact solutions of the one-dimensional one-particle reduction of RLLG for several values of this parameter.

CHAPTER II

WALKS IN RIGID ENVIRONMENTS

2.1 Introduction

Walks in rigid environments (WRE, [10],[11]) are systems generated by the deterministic motion of a particle in an environment of scatterers randomly distributed over the vertices of some graph G. The particle can modify the scattering rules at the vertices lying in its path, according to some deterministic rule. We assume that scatterers of finitely many types are present on the lattice. Then, the basic characteristic of a rigid environment is the *rigidity* function $r : G \to \mathbb{Z}_+$. The value $r(g)$ of this function at a given vertex $g \in G$ is called the local rigidity of the environment at g, which means that the scatterer located at g changes its type after the $r(g)$-th visit of the particle to that vertex. The environment is said to have constant rigidity r if $r(g) = r$ for all $g \in G$.

Models of this type with the extreme values of rigidity: $r = \infty$ or $r = 1$, have been studied extensively even before the notion of rigidity had been introduced. The first case corresponds to the static lattice gas, also referred to as LLG with fixed scatterers, whereas the second case is known as LLG with flipping scatterers, or just flipping LLG (see Chapter I). Walks in rigid environments can be viewed as a generalization of these two models.

This text deals with one-dimensional walks in rigid environments. It has been shown in [10],[11] that one-particle WRE are completely solvable in the case when G is a one-dimensional lattice $\mathbb{Z}$ and the rigidity of the environment is constant. There are four types of scatterers on $\mathbb{Z}$: forward- and back- scatterers which respect the reflection symmetry of $\mathbb{Z}$, and right- and left- rotators which do not. As demonstrated

in [10],[11], WRE formed by either the first or the second pair of scatterers on $\mathbb{Z}$ can exhibit sub-diffusive, diffusive or super-diffusive behaviour. (The last case corresponds to the ultimate propagation on $\mathbb{Z}$ with random velocity). In fact, these systems can be viewed as the simplest, completely solvable, dynamical models of sub-/super-/diffusive motion.

We study continuous limits of these models and derive the corresponding kinetic equations. The results show that, in the limit, the deterministic dynamics prevails over the random fluctuations that are caused by the randomness of the initial distribution of scatterers. This should be contrasted, for example, with the continuous limit of the biased random walk on $\mathbb{Z}$, where the diffusive behaviour emerges on top of the propagation via a proper scaling of transition probabilities (see e.g. [33]). In the WRE under study, no such scaling could be found. The reason for that is the character of evolution in these models. At any moment of time, the environment consists of two parts: the region already visited by the particle and its complement. The deterministic motion in the visited region is intermittent with random excursions to its complement. By virtue of such excursions, the deterministic (already visited) region is growing and, consequently, periods of deterministic motion grow as well, which makes random fluctuations relatively small.

In the last section of this chapter, we present the results of computer simulations of a multi-particle WRE with rigidity 1. Although the corresponding one-particle model has been analyzed in great detail (see [10],[19],[11],[41]) and was shown to be completely solvable, there are no results concerning the multi-particle model as of yet. This can be explained by the fact that rigorous analysis of multi-particle models is generally a lot more complicated than that of single-particle models, due to the particle interactions. We attempt to describe the behaviour of this multi-particle system by studying its statistical properties.

Some of the results presented in this chapter have been published in [14] and [43].

2.2 Definitions

We now give a formal definition of a walk in a rigid environment [10],[11]. A walk in a rigid environment is a dynamical system that is described by the following characteristics:

- a simple regular, undirected, infinite graph G;
- a subset $\hat{S} \subseteq S$ of the scatterers allowed in the model, where S is the set of all possible scatterers on G;
- a function $r : G \to \mathbb{Z}_+$ called the rigidity of the environment;
- a collection of functions $\{e_g\}_{g \in G}$, where each $e_g : \hat{S} \to \hat{S}$ defines the "flipping rule" according to which the scatterer at g changes its type (flips). In other words, it defines the order in which scatterers of different types appear at g.

To say that the environment has constant rigidity r means that the scatterer at vertex $g \in G$ changes its type (flips) after r visits of the particle to this vertex. Note that the evolution of each scatterer is periodic with period r if time is measured in the number of times the particle visits the corresponding vertex. We define the index i of the scatterer at g as the number of visits of the particle to g that have occurred since the last time when this scatterer flipped. Hence, the state of the scatterer at vertex g at any time t is determined by two quantities: the type of scatterer and its index. We define the state function $\eta : G \times \mathbb{Z} \to \Phi_r$ as:

$$\eta(g, t) = (s, i),$$

where $(s, i) \in \Phi_r$, and $\Phi_r = \hat{S} \times \mathbb{Z}_r$ is the set of possible states of a scatterer (the second factor in the product denotes the cyclic group of order r with modulo r addition). After each visit of the particle to g, the state of the scatterer changes according to

the rule given by a function $\phi:\ \Phi_r \to \Phi_r$ which is defined as:

$$\phi(s,i) = \begin{cases} (s, i+1), & \text{if } 0 \le i < r-1, \\ (e_g(s), 0), & \text{if } i = r-1. \end{cases}$$

In the next section, we will introduce two models of walks in rigid environments on $\mathbb{Z}$.

2.3 Finite-Difference Equations

We consider the motion of a single particle on the one-dimensional lattice $\mathbb{Z}$ where each vertex $z \in \mathbb{Z}$ is occupied by a scatterer. The scatterers of finitely many types are distributed independently over all vertices. The particle is moving with unit speed on $\mathbb{Z}$, i.e. $|v(t)| = 1$ at any $t \in \mathbb{Z}$. By $z(t)$, we denote the position of the particle at time t. Without loss of generality, we may assume that the particle starts at the origin: $z(0) = 0$. At each integer time moment it hops from its current position $z(t) \in \mathbb{Z}$ to the neighboring vertex in the direction of its velocity. Upon the particle's visit to a scatterer, both the particle velocity and the state of the scatterer may change. Formally, the dynamics of walks in rigid environments on $\mathbb{Z}$ can be described by the following equations:

$$\begin{aligned} z(t+1) &= z(t) + v(t), \\ v(t+1) &= w_{s(t)}\left(v(t)\right), \\ \eta(z, t+1) &= \begin{cases} \eta(z,t) & \text{if } z \ne z(t), \\ \phi(\eta(z(t),t)) & \text{if } z = z(t). \end{cases} \end{aligned}$$

Here, the function $w_{s(t)}$ is completely defined by the type of scatterer $s(t)$ at position $z(t)$, and can be written explicitly for each model.

The set S of all possible scatterers on $\mathbb{Z}$ consists of the following four types: forward- (FS) and back-scatterers (BS), and right (RR) and left rotators (LR). The forward scatterer corresponds to the trivial case when the velocity vector of the particle does not change upon a collision, i.e. $w_{FS}(v) = v$. The back-scatterer changes

the velocity vector of the particle to the opposite, i.e. $w_{BS}(v) = -v$. The right and left rotators send the scattered particle to the right or to the left respectively, i.e. $w_{RR}(v) = 1$ for the right rotator and $w_{LR}(v) = -1$ for the left rotator. The first pair of scatterers will be referred to as non-oriented scatterers, and the second pair as oriented scatterers. We examine both the model with oriented scatterers (*OS-model*) and the model with non-oriented scatterers (*NOS-model*). In either case the environment is assumed to have constant rigidity.

We derive probabilistic equations governing the dynamics of the particle in OS and NOS models and find the continuous limits of those equations. Since the inverse dynamics is generally not defined and, in this case, only the NOS model has well-defined dynamics for all $t \in \mathbb{Z}$, we only consider $t \geq 0$. To distinguish between the two moments of time just before and just after the particle's interaction with the scatterer, we denote them by t_- and $t_+ \equiv t$ respectively. We assume that the particle starts at the origin with $v(0) = v(0_+) = 1$, and that all scatterers on $\mathbb{Z}$ have index 0 at time $t = 0$. We denote as $f(z, t)$ the probability of finding the particle at position z for the first time at time t. Then we can write down the formula of total probability:

$$f(z + 1, t + 1) = \sum_s a_s f(z, t - t_s) \tag{1}$$

where a_s is the probability that the particle propagates from z to $z + 1$ in $t_s + 1$ time steps, $\sum_s a_s = 1$, and the summation is performed over all possible time delays t_s (i.e. all possible loops that the particle can make between two successive visits to position z). A similar equation can be written for propagation along the negative axis.

Let us take a closer look at the conditions under which equation (1) makes sense. These conditions reflect the hybrid nature of walks in random environments, which are neither purely stochastic nor purely deterministic systems.

At any time instant $t > 0$, the lattice $\mathbb{Z}$ can be divided into two subsets: a subset D_t formed by all vertices $z \in \mathbb{Z}$ visited by the particle to the moment t, and its complement $\bar{D}_t$. Note that the dynamics of the particle in D_t is purely deterministic.

To reflect this, we will call D_t a *deterministic region*. Randomness is introduced into the dynamics when the particle visits vertices in $\bar{D}_t$. Indeed, since the initial distribution of scatterers on $\mathbb{Z}$ is random, then the first visit of the particle to any vertex can be interpreted as a random event. We will refer to $\bar{D}_t$ as a *random region*. Initially, the entire lattice forms a random region: $\bar{D}_0 = \mathbb{Z}$. But once the particle starts moving, a non-trivial deterministic region appears. Generally, $D_0 \subset D_1 \subseteq D_2 \subseteq \ldots \subseteq D_n \subseteq \ldots$. We denote the union of all these deterministic regions as $D_\infty = \cup_t D_t$. Then, for equation (1) to make sense, the following condition has to be satisfied:

Condition I (Unboundedness): D_∞ is unbounded, i.e. the particle never performs periodic motion.

If this condition is not met, then by some finite time t^* (where t^* depends on the initial configuration of scatterers), the particle will have visited all vertices in D_∞ and its motion becomes deterministic. Hence, for $t > t^*$ it does not make sense to speak about the *probability* of finding the particle anywhere on the lattice. For the two models under study, however, the unboundedness of D_∞ has been proven for all $r < \infty$ [10],[11].

In general, equations similar to (1) can be written for propagation along any unbounded path on any graph satisfying the assumptions made at the beginning of Section 2, provided that the particle visits all vertices on this path. In fact, equations of this type have been derived for many probabilistic models. For walks in rigid environments, however, only the probability of the first visit of the particle to a vertex makes sense. Indeed, if the first visit of the particle to position z occurred at some t_z, then for all $t > t_z$, z belongs to the deterministic region, and so, we can no longer speak about the probability of finding the particle at z.

Equation (1) first appeared in [4] with an additional restriction that the sum in the r.h.s. of the equation be over a finite number of possible time delays. We consider a more general class of cellular automata where the summation can be performed over an infinite number of configurations.

In the more general case, when the distance between vertices in $\mathbb{R}$ is ζ, and τ is the elementary time step, the equation for $f(z,t)$ reads [4]:

$$f(z+\zeta, t+\tau) = \sum_s a_s f(z, t - t_s\tau). \tag{2}$$

Here a_s is the probability that the particle propagates from z to $z+\zeta$ in t_s+1 time steps. Again the sum of these probabilities over all possible time delays is 1.

These equations will serve as a basis for deriving specific equations for each of the above models.

2.3.1 NOS Model. Odd Rigidity.

To derive the equation governing the dynamics of the particle in the NOS model, we need to understand what a typical trajectory of the particle looks like (see Figure 1). We define the state of the scatterer at position z at time t as $\eta(z,t) = (s,i)$, where $s \in \{0,1\}$ (0 corresponds to forward-scatterer and 1 to back-scatterer) and $0 \le i < r$.

The finite-difference equation for $r = 1$ has been written in [41]. We derive it here for the sake of completeness. Note that the notion of an index of a scatterer is redundant in this case, because the scatterer flips every time it is hit by the particle. Thus, the state of the scatterer is determined only by its type, i.e. $\eta(z,t) = s$.

Let us suppose that the particle arrives at position z at time t. If $\eta(z,t_-) = 0$, then the particle continues moving with the same velocity $v(t) = v(t_-)$, and arrives at $z+1$ at time $t+1$. The state of the scatterer at z changes to $\eta(z,t_+) = 1$. If $\eta(z,t_-) = 1$ then, at first, the particle is reflected to position $z-1$ and the scatterer at z flips. Upon arriving at $z-1$, however, the particle gets reflected back to position z which is now occupied by the forward scatterer. Hence, the particle continues moving

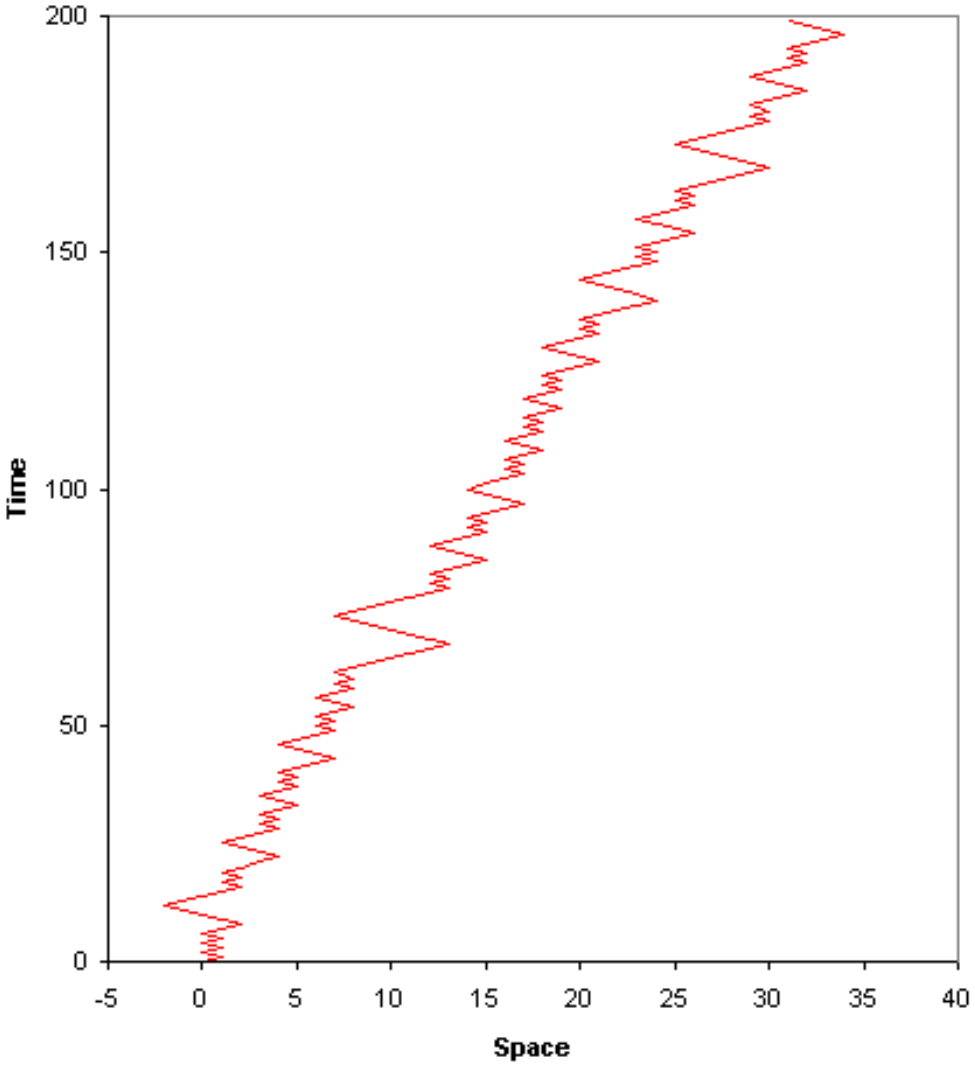

Figure 1: The trajectory of a single particle in the NOS Model with rigidity 3 and $q = 0.5$.

in the positive direction and arrives at $z+1$ at time $t+3$.

Let q denote the concentration of forward scatterers at $t=0$, and $p=1-q$. Then the two possible time delays t_s and their probabilities a_s in equation (1) are given by:

$$\begin{aligned} t_1 &= 0, \qquad a_1 = q, \\ t_2 &= 2, \qquad a_2 = p, \end{aligned} \tag{3}$$

and the first visit equation reads:

$$f(z+1,t+1) = qf(z,t) + pf(z,t-2). \tag{4}$$

Next, we consider the case when $r>1$. Let us suppose that, at time t, the particle arrives at position z for the first time. Depending on the type of scatterer at z, there are two possible outcomes:

If $\eta(z,t_-)=(0,0)$, then after the particle's visit, the state of this scatterer changes to $\eta(z,t_+)=(0,1)$. The particle continues moving with velocity $v(t)=v(t_-)$ and arrives at position $z+1$ at time $t+1$.

If $\eta(z,t_-)=(1,0)$, then, after being reflected by this scatterer, the particle starts traveling in the negative direction until it collides with another back-scatterer, say at position $y<z$ (in fact, $y<z-1$ for all $z>1$). Upon the reflection by this back-scatterer, the particle will bounce between z and y until all scatterers on the interval (y,z) flip and assume state $(1,0)$. Thus, the distance between positions z and y will be covered by the particle $r-1$ times. Meanwhile, the state of the scatterer at position z changes to $(1,(r+1)/2)$. To flip this scatterer and move to the next position on the lattice the particle will have to make an additional $(r+1)/2$ visits to $z-1$. Let $T_{z,z+1}$ denote the time that it takes the particle to propagate from z to $z+1$. Then, the configuration of scatterers at time $t+T_{z,z+1}$ is given by:

$$\begin{aligned} \eta(x,t+T_{z,z+1}) &= (1,0), && y<x<z-1, \\ \eta(z-1,t+T_{z,z+1}) &= \left(1,\tfrac{1}{2}(r+1)\right), \\ \eta(z,t+T_{z,z+1}) &= (0,1). \end{aligned}$$

Remark: Note that between times t and $t + T_{z,z+1}$ the scatterer at position y is visited $(r-1)/2$ times. Hence, this is also the number of times that position $z-1$ will be revisited by the particle if, in the course of propagation, it encounters another back-scatterer.

This describes the typical trajectory of the particle propagating from z to $z+1$. The only exception to this general rule is the propagation from position 1 to position 2 when the scatterers at positions 0 and 1 are both in the state (1,0). In this case, upon arriving at $z = 1$ for the first time at $t = 1$, the particle simply bounces between 0 and 1 until *both* scatterers flip. It arrives at position 2 after $T_{1,2} = 2r+1$ time steps. After this, its trajectory follows the general rule described above. The configuration of scatterers resulting from the propagation of the particle from position 1 to position 2 is given by:

$$\begin{aligned} \eta(0, 1 + T_{1,2}) &= (0, 0), \\ \eta(1, 1 + T_{1,2}) &= (0, 1). \end{aligned}$$

Remark: Note that in the course of propagation, the scatterer at position 0 is visited r times instead of the typical $(r-1)/2$.

We are ready now to compute the time delays t_s in the equation (1), and the probabilities a_s with which they occur. We start with $\eta(z, t_-) = (1, 0)$. Let d be the random variable that corresponds to the distance between z and the position y of the back-scatterer closest to z with $y < z$, at time t. Note that, if $z > 1$, then $\eta(z-1, t) = (0, 1)$. Hence, $y < z-1$ and d is bounded from below by 2.

It follows from the description of a typical trajectory that the time required for the particle to propagate from z to $z+1$, for each $d = j$, is equal to

$$t_j = (r-1)j + (r+1), \quad j \geq 2. \tag{5}$$

The corresponding probabilities $a_j = \mathcal{P}\{d = j\}$ can be computed as follows:

$$a_j = \mathcal{P}\left\{\eta(z,t) = (1,*);\ \eta(z-j,t) = (1,*);\ \eta(n,t) = (0,*), z-j < n < z\right\} =$$

$$= \begin{cases} \mathcal{P}\{\eta(z,0) = \eta(z-j+1,0) = (1,0); & \\ \qquad \eta(n,0) = (0,0), z-j+1 < n < z\}, & 2 \le j \le z-1; \\ & \\ \mathcal{P}\{\eta(z,0) = \eta(1,0) = (1,0); & \\ \qquad \eta(n,0) = \eta(0,0) = (0,0), 1 < n < z\} + & j = z; \\ +\mathcal{P}\{\eta(z,0) = \eta(0,0) = (1,0); & \\ \qquad \eta(n,0) = (0,0), 0 < n < z\}, & \\ & \\ \mathcal{P}\{\eta(z,0) = \eta(z-j,0) = (1,0); & \\ \qquad \eta(n,0) = (0,0), z-j < n < z\} + & j \ge z+1. \\ +\mathcal{P}\{\eta(z,0) = \eta(z-j,0) = \eta(0,0) = \eta(1,0) = (1,0); & \\ \qquad \eta(n,0) = (0,0), z-j < n < z, n \ne 0,1\}, & \end{cases} \tag{6}$$

where $*$ denotes *any* index between 0 and $r-1$.

If, on the other hand, position z is occupied by a forward scatterer at time t_-, i.e. $\eta(z,t_-) = (0,0)$, then there is no time delay in propagation from z to $z+1$. Conforming to the notations used in equation (1), we assign subscript $j = 1$ to the quantities corresponding to this case. Thus,

$$t_1 = 0 \quad \text{and} \quad a_1 = \mathcal{P}\{\eta(z,t) = (0,*)\} \tag{7}$$

Since the initial distribution of scatterers among the lattice vertices was independent, we can easily rewrite the equations for a_j, $j \ge 1$, in terms of initial concentrations of back- and forward- scatterers p and q:

$$a_j = \begin{cases} q, & j = 1; \\ p^2 q^{j-2}, & 2 \le j \le z-1; \\ p^2 q^{j-1} + p^2 q^{j-1} = 2p^2 q^{j-1}, & j = z; \\ p^2 q^{j-1} + p^4 q^{j-3} = p^2(p^2+q^2) q^{j-3}, & j \ge z+1. \end{cases} \tag{8}$$

It is easy to verify that $\sum_j a_j = 1$.

Now, combining equations (1), (7) and (8) we obtain the first-visit equation for the NOS model with odd rigidity:

$$f(z+1, t+1) = qf(z,t) + \sum_{j=2}^{\infty} a_j f(z, t-t_j); \tag{9}$$

where time delays t_j are given by formula (5) and the corresponding probabilities a_j by formula (8).

2.3.2 NOS Model. Even Rigidity

Of all models under study, this is the most complicated one in terms of the particle's dynamics. We begin by describing a typical trajectory of the particle for a given initial configuration of scatterers (see Figure 2). Let d_i, $i = 1, 2, \ldots$ denote the positions of back-scatterers on $\mathbb{Z}_+$ at time $t = 0$. We assume $d_0 = 0$. Let t_i be the times of the particle's first visits to positions d_i, $i = 1, 2, \ldots$. As before, $\eta(z,t) = (s,i)$ shall denote the state of the scatterer at position z at time t.

The first-visit equation will be derived for $z > 0$. The case of negative z can be considered in a similar way. Let us suppose that, at time t, the particle arrives at position z for the first time.

If $\eta(z, t_-) = (0,0)$, then after the particle's collision with the scatterer, the state of the scatterer changes to $\eta(z, t_+) = (0,1)$. The particle continues moving with velocity $v(t) = v(t_-)$ and arrives at position $z+1$ at time $t+1$.

If $\eta(z, t_-) = (1,0)$, i.e. position z is occupied by a back-scatterer, then, according to the notations introduced earlier, $z = d_l$ and $t = t_l$ for some l, $1 \le l \le z$. The

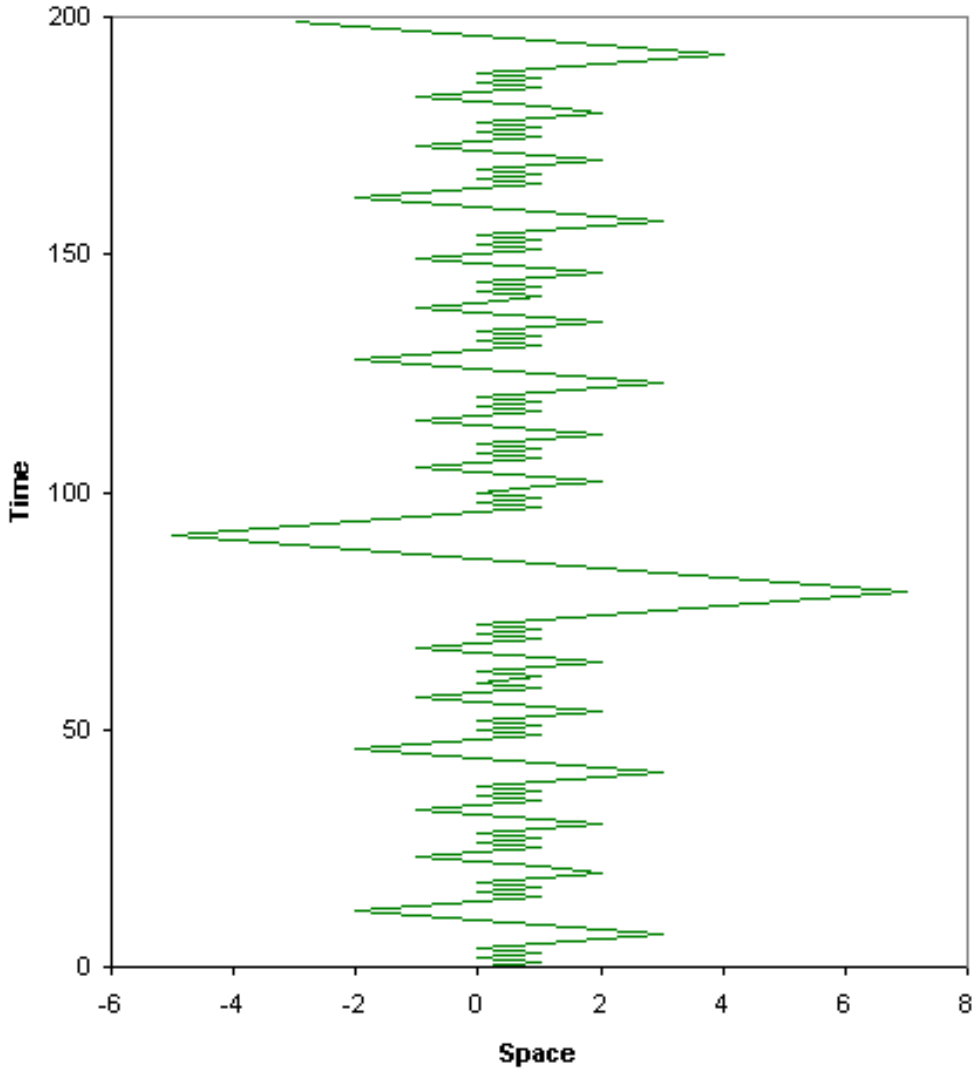

Figure 2: The trajectory of a single particle in the NOS Model with rigidity 2 and $q = 0.5$.

precise trajectory of the particle depends on several factors, including the type of scatterer at the origin at time $t = 0$. However, neither the general pattern of the particle's motion, nor the final equation are affected by this factor. Hence, it suffices to describe the typical trajectory only in the case $\eta(0,0) = (0,0)$. In the course of propagation from z to $z+1$, the particle performs a series of steps described below.

Let us denote as y_k the position of the back-scatterer closest to $-k+1$ such that $y_k < -k+1$. Then during the first step, the particle bounces on the interval $[y_{d_{l-1}}, z]$ covering the length of $[0, z]$ $(r-1)$ times and the length of $[y_{d_{l-1}}, 0]$ r times.

In step 2, it bounces on the intervals [0,1] and [-1,2] covering the length of [0,1] $2r$ times and the length of [-1,2] r times.

During each subsequent step i, the particle bounces on intervals [0,1], [-1,2], ..., $[-i, i+1]$, $i < z-1$ covering the length of [0,1] $2r$ times and the lengths of all other intervals r times.

In $(z-1)$-st step, the behaviour of the particle depends on the state of the scatterer at position $-z+1$. If $\eta(-z+1, t_l) = (1,0)$ or $(1, r/2)$, then during this step it bounces on [0,1], ...,$[-z+1, z]$ following the above pattern. If $\eta(-z+1, t_l) = (0,0)$, then it bounces on [0,1], ..., $[-z+2, z-1]$, $[y_z, z]$ instead, where y_z is defined as above.

After this, the particle returns to z and repeats the same series of steps once again with minor or no changes to all but the last step. The sequence of the intervals involved in this last step again depends on $\eta(-z+1, t_l)$. If $\eta(-z+1, t_l) = (1,0)$ or $(0,0)$, then the particle bounces on intervals [0,1], [-1,2], ..., $[-z+1, z]$, and if $\eta(-z+1, t_l) = (1, r/2)$, then it bounces on [0,1], ..., $[-z+2, z-1]$, $[y_z, z]$. Upon finishing this step, the particle proceeds directly to $z+1$.

To compute the delay times t_s, notice that during its propagation from z to $z+1$, the particle covers the length of each interval $[-i+1, i]$ exactly $(2r)2^{z-i}$ times for $i = 2, \ldots, z$ and the length of $[y_z, -z+1]$ r times. The length of [0,1] is covered $2\sum_{i=2}^{z}(2r)2^{z-i} = 4r(2^{z-1}-1)$ times. Let d be the random variable corresponding to

the distance between $(-z+1)$ and y_z. Then, for any $d=j$, the delay time t_j can be computed as follows:

$$\begin{aligned} t_j &= \sum_{i=2}^{z} 2r2^{z-i}(2i-1) + 4r(2^{z-1}-1) + rj = \\ &= r(j + 7\cdot 2^z - 4z - 10), \qquad\qquad j \geq 0. \end{aligned} \tag{10}$$

It follows from the description of the trajectory, that time delay t_j, $j \geq 1$ occurs if the distance between $(-z+1)$ and y_z is equal to j and $\eta(-z+1,t) \neq (1,0)$, whereas time delay t_0 occurs when $\eta(-z+1,t) = (1,0)$. If we denote the probability of the event that $\eta(-z+1,t) = (1,0)$ as $\mathcal{P}_{(1,0)}$, then

$$\begin{aligned} a_0 &= p\mathcal{P}_{(1,0)}, \\ a_j &= p^2 q^{j-1}(1-\mathcal{P}_{(1,0)}), \quad j \geq 1. \end{aligned} \tag{11}$$

To compute these probabilities, we need to compute the value of $\mathcal{P}_{(1,0)}$. To do so, we compute it for an arbitrary configuration of scatterers at time $t=0$, and then perform the summation over all possible configurations with appropriate weights. Let $\mathcal{P}^l_{(1,0)}(d_1,\ldots,d_l)$ denote the conditional probability of the event that $\eta(-z+1,t) = (1,0)$ given that at $t=0$ positions d_i, $1 \leq i \leq l$ are occupied by back-scatterers, and $z=d_l$, $t=t_l$ for some $1 \leq l \leq z$. The scatterer at position $(-z+1)$ will be in state (1,0) at time t in one of the two cases:

- if $\eta(-z+1,0) = (0,0)$, and the scatterer has been visited by the particle some time before t_l. Note that it could have been visited during any of the time intervals $[t_{i-1},t_i)$, $2 \leq i \leq l$ ($t_1 = 1$ for any configuration of scatterers, so the particle does not escape from [0,1] during time interval $[t_0,t_1)$);
- if $\eta(-z+1,0) = (1,0)$, and the scatterer has not been visited before time t_l.

The probability of the event that $(-z+1)$ was visited during time interval $[t_{i-1},t_i)$ is equal to:

$$\begin{aligned} \mathcal{P}\{\eta(k,0) = (0,0),\ -d_l+2 \leq k \leq -d_{i-1};\ \eta(-d_{i-1}+1,t_{i-1}) \neq (1,0)\} = \\ = q^{d_l - d_{i-1} - 1}(1 - \mathcal{P}^{i-1}_{(1,0)}(d_1,\ldots,d_{i-1})). \end{aligned}$$

Hence, the total probability $\mathcal{P}_v(d_1,\ldots,d_l)$ of the event that the scatterer at $(-z+1)$ has been visited before time t_l can be computed as a sum of the above probabilities over all time intervals $[t_{i-1},t_i)$:

$$\mathcal{P}_v(d_1,\ldots,d_l)=\sum_{i=2}^{l} q^{d_l-d_{i-1}-1}(1-\mathcal{P}^{i-1}_{(1,0)}(d_1,\ldots,d_{i-1})).$$

Now, the probability $\mathcal{P}^l_{(1,0)}(d_1,\ldots,d_l)$ can be computed as follows:

$$\begin{aligned}\mathcal{P}^l_{(1,0)}(d_1,\ldots,d_l) &= q\mathcal{P}_v(d_1,\ldots,d_l)+p(1-\mathcal{P}_v(d_1,\ldots,d_l))= \\ &= p+(q-p)\sum_{i=2}^{l} q^{d_l-d_{i-1}-1}(1-\mathcal{P}^{i-1}_{(1,0)}(d_1,\ldots,d_{i-1})),\quad 2\le l\le z, \\ \mathcal{P}^1_{(1,0)}(d_1) &= p.\end{aligned} \tag{12}$$

This is a recursive equation for $\mathcal{P}^l_{(1,0)}(d_1,\ldots,d_l)$. To solve it, it is convenient to define a new quantity $B_i=q^{-d_i-1}(1-\mathcal{P}^i_{(1,0)}(d_1,\ldots,d_i))$. The equations for B_l follow immediately from (12):

$$\begin{cases} B_l = q^{-d_l}+\left(\dfrac{p}{q}-1\right)\displaystyle\sum_{i=1}^{l-1} B_i, \quad 2\le l\le z, \\ B_1 = q^{-d_1}. \end{cases} \tag{13}$$

The following sequence of equations allows us to find the solution of this system. Each equation of the sequence was obtained by applying (13) to the last term of the sum appearing in the preceding step.

$$\begin{aligned}\sum_{i=1}^{l} B_i &= q^{-d_l}+\frac{p}{q}\sum_{i=1}^{l-1} B_i = \\ &= q^{-d_l}+\frac{p}{q}\left(q^{-d_{l-1}}+\frac{p}{q}\sum_{i=1}^{l-2} B_i\right)= \\ &\qquad\qquad \ldots \\ &= q^{-d_l}+\frac{p}{q}\left(q^{-d_{l-1}}+\frac{p}{q}\left(q^{-d_{l-2}}+\ldots+\frac{p}{q}\left(q^{-d_2}+\frac{p}{q}B_1\right)\ldots\right)\right)= \\ &= \sum_{j=0}^{l-1}\left(\frac{p}{q}\right)^j q^{-d_{l-j}} = \sum_{i=1}^{l}\left(\frac{p}{q}\right)^{l-i} q^{-d_i}.\end{aligned}$$

Hence, the solution of (13) is given by:

$$B_l = q^{-d_l}+\left(\frac{p}{q}-1\right)\sum_{i=1}^{l-1}\left(\frac{p}{q}\right)^{l-i-1} q^{-d_i}.$$

Going back to $\mathcal{P}^l_{(1,0)}(d_1,\ldots,d_l)$, we get:

$$\mathcal{P}^l_{(1,0)}(d_1,\ldots,d_l) = \begin{cases} p, & l=1, \\ p-(p-q)\sum_{i=2}^{l}\left(\frac{p}{q}\right)^{l-i} q^{d_l-d_{i-1}}, & 2\le l\le z. \end{cases} \tag{14}$$

Finally, to compute $\mathcal{P}_{(1,0)}$, we sum the probabilities given by (14) over all possible configurations of scatterers:

$$\begin{aligned} \mathcal{P}_{(1,0)} &= \sum_{l=1}^{z} p^l q^{z-l} \sum_{1\le d_1<\ldots<d_{l-1}<d_l=z} \mathcal{P}^l_{(1,0)}(d_1,\ldots,d_l) = \\ &= p^2 q^{z-1} + \sum_{l=2}^{z} p^l q^{z-l} \sum_{1\le d_1<\ldots<d_{l-1}<d_l=z} \left(p-(p-q)\sum_{i=2}^{l}\left(\frac{p}{q}\right)^{l-i} q^{d_l-d_{i-1}}\right) = \\ &= p^2 q^{z-1} + \sum_{l=2}^{z} p^l q^{z-l} \left(p\, C^{l-1}_{z-1} - (p-q)\sum_{i=2}^{l}\left(\frac{p}{q}\right)^{l-i} \sum_{1\le d_1<\ldots<d_{l-1}<d_l=z} q^{d_l-d_{i-1}}\right), \end{aligned}$$

where the last equality was obtained by using the following identity:

$$\sum_{1\le d_1<\ldots<d_{l-1}<d_l=z} 1 = C^{l-1}_{z-1}. \tag{15}$$

The sum on the l.h.s. of (15) is simply the number of possible configurations of scatterers, where exactly $(l-1)$ vertices of the lattice interval $[1, z-1]$ are occupied by back scatterers.

Next, we compute the sum over all qualified configurations of scatterers $\{d_1,\ldots,d_l\}$ in $\mathcal{P}_{(1,0)}$, using the fact that the scatterers were initially placed in the lattice vertices independently:

$$\begin{aligned} \sum_{1\le d_1<\ldots<d_{l-1}<d_l=z} q^{d_l-d_{i-1}} &= q^z \sum_{n=i-1}^{z-(l-i+1)} \sum_{1\le d_1<\ldots<d_{i-2}<n<d_i<\ldots<d_l=z} q^{-n} = \qquad (n=d_{i-1}) \\ &= q^z \sum_{n=i-1}^{z-(l-i+1)} \sum_{1\le d_1<\ldots<d_{i-2}<n} \sum_{n<d_i<\ldots<d_l=z} q^{-n} = \\ &= q^z \sum_{n=i-1}^{z-(l-i+1)} C^{i-2}_{n-1}\, C^{l-i}_{z-n-1}\, q^{-n}. \end{aligned}$$

The last equality was obtained by applying identity (15) to the two internal sums. Substituting the result of this computation into the expression for $\mathcal{P}_{(1,0)}$ above and

subsequently changing the summation order in the obtained expression yields:

$$\begin{aligned}\mathcal{P}_{(1,0)} &= \sum_{l=1}^{z} C_{z-1}^{l-1} p^{l+1} q^{z-l} - (p-q) \sum_{l=2}^{z} \sum_{i=2}^{l} p^{2l-i} q^{2(z-l)+i} \sum_{n=i-1}^{z-(l-i+1)} C_{n-1}^{i-2}\, C_{z-n-1}^{l-i}\, q^{-n} = \\ &= p^2 (p+q)^{z-1} - (p-q) \sum_{n=1}^{z-1} \sum_{i=2}^{n+1} C_{n-1}^{i-2} q^{-n} \sum_{l=i}^{z-n+i-1} C_{z-n-1}^{l-i} p^{2l-i} q^{2(z-l)+i}.\end{aligned}$$

Then, computing the sum over l:

$$\begin{aligned}\sum_{l=i}^{z-n+i-1} C_{z-n-1}^{l-i} p^{2l-i} q^{2(z-l)+i} &= p^i q^{-i} \sum_{j=0}^{z-n-1} C_{z-n-1}^{j} p^{2j} q^{2(z-j)} = && (j=l-i) \\ &= p^i q^{2n+2-i} (p^2+q^2)^{z-n-1},\end{aligned}$$

and using the identity $p+q=1$, we obtain:

$$\begin{aligned}\mathcal{P}_{(1,0)} &= p^2 - (p-q) \sum_{n=1}^{z-1} (p^2+q^2)^{z-n-1} \sum_{i=2}^{n+1} C_{n-1}^{i-2} p^i q^{n+2-i} = \\ &= p^2 - (p-q) \sum_{n=1}^{z-1} (p^2+q^2)^{z-n-1} \sum_{m=0}^{n-1} C_{n-1}^{m} p^{m+2} q^{n-m} = && (m=i-2) \\ &= p^2 - (p-q) \sum_{n=1}^{z-1} (p^2+q^2)^{z-n-1} (p+q)^{n-1} = \\ &= p^2 - (p-q) p^2 q \sum_{j=0}^{z-2} (p^2+q^2)^j = && (j=z-n-1) \\ &= p^2 - p^2 q (p-q) \frac{1-(p^2+q^2)^{z-1}}{1-p^2-q^2}.\end{aligned}$$

Using the identity $p+q=1$ here once again, we arrive at the following expression for $\mathcal{P}_{(1,0)}$:

$$\mathcal{P}_{(1,0)} = \frac{p}{2} + \frac{p}{2}(p-q)\left(p^2+q^2\right)^{z-1}. \tag{16}$$

Now, having computed $\mathcal{P}_{(1,0)}$, the probabilities a_j, $j \geq 0$, are given by equations (11).

In the case when $\eta(z, t_-) = (0,0)$, there is no time delay, and the corresponding probability equals the probability of the event that $\eta(z,0) = (0,0)$. In order to conform to the notations used in (1), we assign index (-1) to the quantities corresponding to this case, i.e.:

$$t_{-1} = 0, \quad \text{and} \quad a_{-1} = q. \tag{17}$$

It is easy to verify that $a_{-1} + \sum_{j\geq 0} a_j = 1$.

We are now ready to write the first visit equation for the NOS model with even rigidity for $z > 0$. Combining equations (1), (11) and (17) we obtain:

$$\begin{aligned} f(z+1,t+1) = \; & qf(z,t) + p\mathcal{P}_{(1,0)} f(z,t-t_0) \\ & + p^2(1-\mathcal{P}_{(1,0)}) \sum_{j=1}^{\infty} q^{j-1} f(z,t-t_j), \end{aligned} \tag{18}$$

where probability $\mathcal{P}_{(1,0)}$ is given by (16) and time delays t_j by (10). A similar equation can be obtained for $z < 0$.

2.3.3 OS Model.

Again, we begin with the description of a typical trajectory of the particle in the OS model (see Figure 3). We still use the same notation $\eta(z,t) = (s,i)$ for the state of the scatterer occupying position z at time t. Now, however, $s = 0$ corresponds to a right rotator and $s = 1$ to a left rotator. Let L_z, $z > 0$, be the random variable corresponding to the number of left rotators on the interval $[1, z]$ at time $t = 0$, and R_z, $z \leq 0$, be the random variable corresponding to the number of right rotators on the interval $[z, 0]$.

Let us suppose that, at time t, the particle arrives at position $z > 0$ for the first time. Then, depending on the type of scatterer at this vertex, there are two possible outcomes.

If $\eta(z, t_-) = (0,0)$, then after the particle's collision with the scatterer, the state of the scatterer changes to $\eta(z, t_+) = (0,1)$. The particle proceeds directly to $z+1$ and arrives there at time $t+1$.

If $\eta(z, t_-) = (1,0)$, then the particle gets reflected by the scatterer at z. Next, due to the presence of the right rotator at $z-1$ (the particle passed through it in the previous step), it will bounce between positions z and $z-1$ until this rotator flips. At the time of flipping the particle will have covered the distance between the two positions $(2r-1)$ times and will be located at $z-1$.Thus, it will be sent further to the left. A similar process takes place on each of the intervals $[z-2, z-1]$,...,$[1,2]$. After

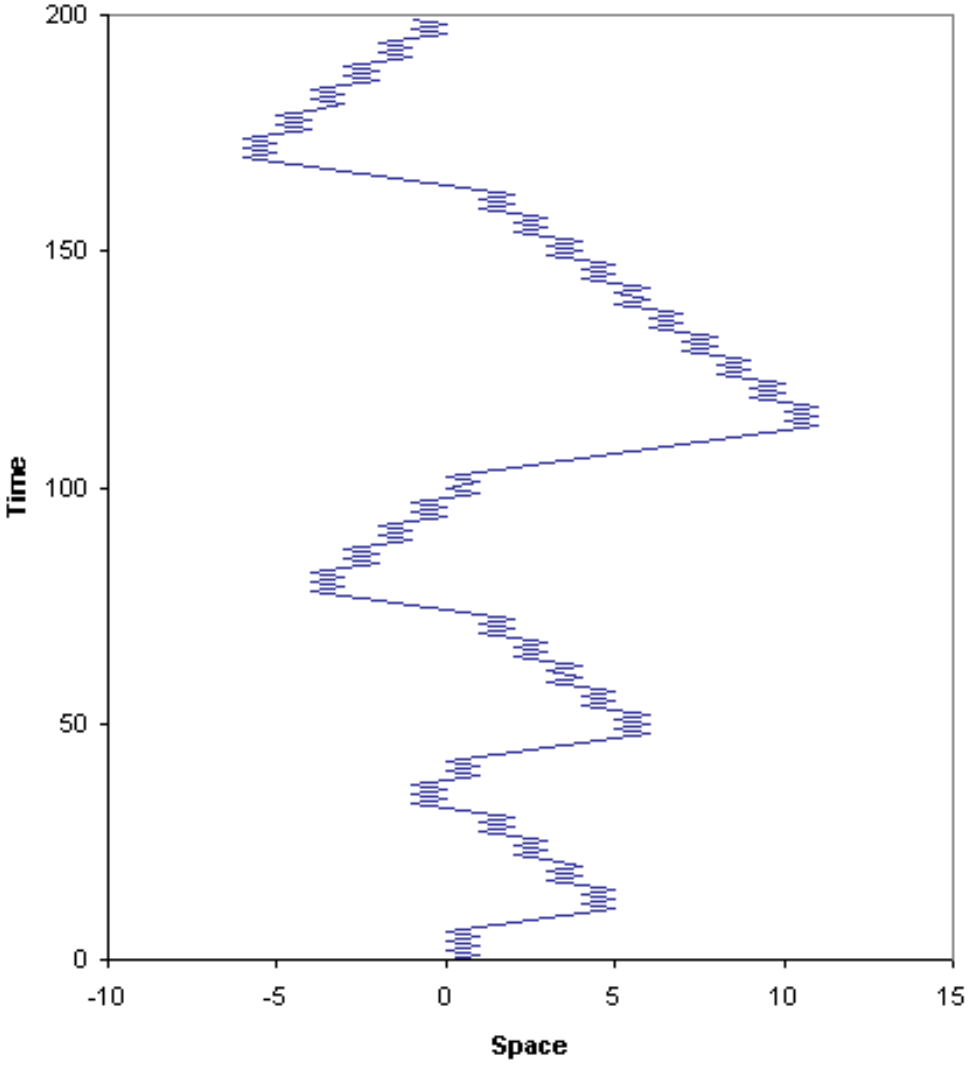

Figure 3: The trajectory of a single particle in the OS Model with rigidity 3 and $q = 0.5$.

returning to position 1, it will be scattered to the left once again, where it travels to the nearest position $y \leq 0$ with $R_y = L_z$ and $\eta(y,t) = (0,0)$. Since y is occupied by the right rotator, the particle will be reflected to the right. Next, it will bounce on each of the intervals $[y, y+1]$,$[y+1, y+2]$,...,$[0,1]$ in the same way it did on the positive semiaxis. After returning to position 1 it will travel directly to position $z+1$. If $T_{z,z+1}$ is the time it takes for the particle to propagate from z to $z+1$, then the configuration of scatterers after $T_{z,z+1}$ time steps is given by:

$$\begin{aligned} \eta(x, t+T_{z,z+1}) &= (1,0), \quad y \leq x \leq 0, \\ \eta(x, t+T_{z,z+1}) &= (0,1), \quad 1 \leq x \leq z. \end{aligned}$$

Note that, in the course of propagation, the particle covers the length of each interval $[i, i+1]$, $y \leq i \leq z-1$, $2r$ times.

Let us compute the time delays t_s in the equation (1) and their probabilities a_s, starting with the case $\eta(z, t_-) = (1,0)$. For each $L_z = l$, $1 \leq l \leq z$, let d_l be the random variable that corresponds to the distance between position $y \leq 0$, such that $R_y = l$ and $\eta(y,0) = (0,0)$, and the origin. Note that $d_l \geq l-1$. It follows from the observation above that the extra time it takes for the particle to propagate from z to $z+1$, for each $d_l = j$ is equal to

$$t_{lj} = 2r(z+j), \quad j \geq l-1. \tag{19}$$

This delay occurs if, at time $t=0$, there were exactly $l-1$ right scatterers on the interval $[-(j-1), 0]$, and $\eta(-j, 0) = (0,0)$. There are C_j^{l-1} such configurations for each l. The probability of the event that $L_z = l$ is equal to the probability that there were exactly $l-1$ left scatterers on the interval $[1, z-1]$ at $t=0$, and $\eta(z,0) = (1,0)$. Let q denote the concentration of right rotators at time $t=0$, and $p = 1-q$, then the probability of delay t_{lj} is given by

$$a_{lj} = (C_{z-1}^{l-1} p^l q^{z-l})(C_j^{l-1} q^l p^{j+1-l}), \;\; 1 \leq l \leq z, \;\; j \geq l-1. \tag{20}$$

In order to be consistent with the notations used in equation (1), we assign index $s = 0$ to the quantities associated with the case when $\eta(z,t) = (0,0)$. Then

$$t_0 = 0, \text{ and } a_0 = q. \tag{21}$$

It can be verified that $a_0 + \sum_{l=1}^{z} \sum_{j \geq l-1} a_{lj} = 1$.

Now, we can combine equations (1) and (19)-(21) to write the first-visit equation for the OS model for $z > 0$:

$$f(z+1,t+1) = qf(z,t) + \sum_{l=1}^{z} \sum_{j=l-1}^{\infty} C_{z-1}^{l-1} C_j^{l-1} q^z p^{j+1} f(z, t-2r(z+j)). \tag{22}$$

Changing the order of summation and computing the internal sum in the resulting equation reduces (22) to:

$$f(z+1,t+1) = qf(z,t) + \left(\frac{q}{p}\right)^z \sum_{k=z}^{\infty} C_{k-1}^{z-1} p^{k+1} f(z, t-2rk), \tag{23}$$

where the new index of summation k is related to the old index j via $k = j + z$.

The equation for $z \leq 0$ can be obtained in the same way as it was done for positive z and reads:

$$f(z-1,t+1) = pf(z,t) + \left(\frac{p}{q}\right)^{|z|+2} \sum_{k=|z|+2}^{\infty} C_{k-1}^{|z|+1} q^{k+1} f(z, t-2rk). \tag{24}$$

2.4 Continuous Limits

Let us consider equation (2), which is a slightly more general version of equation (1), where the distance between neighboring vertices on $\mathbb{R}$ is ζ and the elementary time step is τ. The distribution function of time delays in the model described by this equation allows us to define the following two quantities [5]: the average displacement time (the average time taken by the particle to perform a displacement from z to $z+\zeta$)

$$\langle t_D \rangle = \sum_s a_s (t_s + 1)\tau = \tau \left(\langle t_s \rangle + 1 \right),$$

and the variance

$$\mathrm{Var}(t_D) = \langle (t_s+1)^2 \rangle \tau^2 - \langle t_D \rangle^2 = \tau^2 \left(\langle t_s^2 \rangle - \langle t_s \rangle^2 \right).$$

In order to find the continuous limit of the finite-difference equation (1) we can expand equation (2) in powers of ζ and τ, and then pass to the limit $\zeta, \tau \to 0$. Expanding (2) in powers of ζ and τ and making use of the identity $\sum_s a_s = 1$, we obtain:

$$\partial_z f(z,t)\zeta + \partial_t f(z,t)\langle t_D\rangle + \\ + \frac{1}{2}\left(\partial_z^2 f(z,t)\zeta^2 + 2\partial_z\partial_t f(z,t)\zeta\tau + \partial_t^2 f(z,t)\tau^2 - \partial_t^2 f(z,t)\sum_s a_s t_s^2 \tau^2\right) + h.o.t. = 0$$

Using iteration, we can substitute spatial derivatives in the terms that contain $\partial_z^2 f(z,t)$ and $\partial_z\partial_t f(z,t)$ with their expressions in terms of time derivatives:

$$\partial_z f(z,t)\zeta = -\partial_t f(z,t)\langle t_D\rangle + h.o.t.$$

The resulting equation reads:

$$\partial_z f(z,t)\zeta + \partial_t f(z,t)\langle t_D\rangle - \frac{1}{2}\partial_t^2 f(z,t)\mathrm{Var}(t_D) + h.o.t. = 0,$$

and in the limit $\zeta, \tau \to 0$ reduces to:

$$\partial_z f(z,t) + \frac{1}{c}\partial_t f(z,t) = \frac{\gamma}{2}\partial_t^2 f(z,t), \tag{25}$$

where

$$\frac{1}{c} = \lim_{\zeta\to 0,\tau\to 0}\frac{\langle t_D\rangle}{\zeta}, \quad \gamma = \lim_{\zeta\to 0,\tau\to 0}\frac{\mathrm{Var}(t_D)}{\zeta}, \tag{26}$$

and the limit $\zeta, \tau \to 0$ is subject to the condition that both γ and $1/c$ be finite. This equation was first written in [5] under the assumption that the summation in (1) is performed over a finite number of configurations. Note, however, that the form of equation (25) does not depend on whether the summation is performed over a finite or an infinite number of configurations.

2.4.1 NOS Model. Odd rigidity

The time delays t_j and their probabilities a_j in the model with $\zeta = 1$ and $\tau = 1$ have been computed in the preceding section. In order to obtain the corresponding

quantities for the case of arbitrary ζ and τ, let us make two observations. First, the quantities t_j, computed earlier, represent the number of *time steps* that it takes the particle to flip the scatterer at position z and start moving to the next position on the lattice. Thus, the values of t_j, $j \geq 1$, in (5) and (7) do not depend on the value of the elementary time step τ and, therefore, are valid for any τ. Second, for $r = 1$ the probabilities a_j given by (3) do not depend on the distance between lattice vertices. Hence, they also stay the same after the rescaling. For the case $r > 1$, however, we need to replace z with $N = z/\zeta$ in the formula for a_j, as N represents the number of lattice unit lengths between the vertex with coordinate z and the origin for an arbitrary ζ. The values of a_j for this case are given by

$$a_j = \begin{cases} q, & j = 1; \\ p^2 q^{j-2}, & 2 \leq j \leq N-1; \\ p^2 q^{j-1} + p^2 q^{j-1} = 2p^2 q^{j-1}, & j = N; \\ p^2 q^{j-1} + p^4 q^{j-3} = p^2(p^2+q^2)q^{j-3}, & j \geq N+1. \end{cases}$$

Note that in the limit $\zeta \to 0$, N becomes unbounded.

The computations of $\langle t_D \rangle$ and $\mathrm{Var}(t_D)$ are fairly straightforward and shall be omitted here for the sake of brevity. The results are presented below:

$$\begin{aligned} \langle t_D \rangle &= \tau \left(r(1+2p) + \mathcal{O}(Nq^N) \right), \\ \mathrm{Var}(t_D) &= \tau^2 \frac{q}{p} \left((r(1+2p)-1)^2 + (r-1)^2 + \mathcal{O}(N^2 q^N) \right), \quad \text{as } N \to \infty. \end{aligned}$$

These formulae are valid for any odd $r \geq 1$.

This allows us to compute c and γ in equation (25). Substituting the values obtained for $\langle t_D \rangle$ and $\mathrm{Var}(t_D)$ into (26) and taking the limit $\zeta \to 0$, $\tau \to 0$ yields:

$$\begin{aligned} \frac{1}{c} &= r(1+2p) \lim_{\zeta \to 0, \tau \to 0} \frac{\tau}{\zeta}, \\ \gamma &= \frac{q}{p} \left((r(1+2p)-1)^2 + (r-1)^2 \right) \lim_{\zeta \to 0, \tau \to 0} \frac{\tau^2}{\zeta}. \end{aligned}$$

The condition of boundedness of both of these quantities requires that $\lim_{\zeta \to 0, \tau \to 0}(\tau/\zeta)$

be finite. We choose

$$\lim_{\zeta\to 0,\tau\to 0}\frac{\tau}{\zeta}=1$$

to preserve the scaling factor of 1 obtained in the case when $\zeta=\tau=1$. Clearly, under this condition, $\gamma=0$, so the continuous limit of the equation (9) reads:

$$\partial_z f(z,t)+r(1+2p)\partial_t f(z,t)=0. \tag{27}$$

This equation describes propagation on the real line with speed $(r(1+2p))^{-1}$. Since the expected value of the particle's position is proportional to time, its second moment grows quadratically. Therefore, in the continuous limit, the NOS model with odd rigidity exhibits a super-diffusive behaviour.

2.4.2 NOS Model. Even Rigidity

The time delays t_j and their probabilities a_j for the case of an arbitrary ζ and τ can be obtained from (10)-(11) by substituting z with $N=z/\zeta$, as we did before. Hence, for $z>0$ we have

$$t_j = \begin{cases} 0, & j=-1,\\ r(j+7\cdot 2^N-4N-10), & j\geq 0,\end{cases}$$

$$a_j = \begin{cases} q, & j=-1,\\ p\,\mathcal{P}_{(1,0)}, & j=0,\\ p^2q^{j-1}(1-\mathcal{P}_{(1,0)}), & j\geq 1,\end{cases}$$

where

$$\mathcal{P}_{(1,0)}=\frac{p}{2}+\frac{p}{2}(p-q)\left(p^2+q^2\right)^{N-1}.$$

Using these formulae, we can compute the average displacement time and its variance:

$$\begin{aligned}\langle t_D\rangle &= \tau(7rp\,2^N+\mathcal{O}(N)),\\ \mathrm{Var}(t_D) &= \tau^2(49r^2p\,q\,2^{2N}+\mathcal{O}(N2^N)),\quad \text{as } N\to\infty.\end{aligned}$$

Dividing these by ζ and taking the limit $\zeta \to 0$, $\tau \to 0$, we find the coefficients in equation (25):

$$\begin{aligned} \frac{1}{c} &= 7rp \lim_{\zeta\to 0,\tau\to 0} \frac{2^{z/\zeta}\tau}{\zeta}, \\ \gamma &= 49r^2 p\, q \lim_{\zeta\to 0,\tau\to 0} \frac{2^{2z/\zeta}\tau^2}{\zeta}. \end{aligned}$$

The condition of boundedness of these quantities requires that both limits in the above expressions be finite. Since z enters the above limits exponentially we choose

$$\lim_{\zeta\to 0,\tau\to 0} \frac{2^{z/\zeta}\tau}{\zeta} = 2^z$$

or, equivalently, $\tau = \mathcal{O}(\zeta\, 2^{-z/\zeta})$. Under this condition $\gamma = 0$, $1/c = 7rp\, 2^z$ and the continuous limit of the equation (18) for $z > 0$ reads:

$$\partial_z f(z,t) + 7rp\, 2^z \partial_t f(z,t) = 0. \tag{28}$$

Similarly, one can show that the continuous limit of the kinetic equation corresponding to the case $z \leq 0$ is given by

$$\partial_z f(z,t) - 7rp\, 2^{|z|} \partial_t f(z,t) = 0. \tag{29}$$

This equation can also be obtained by changing the sign of z in equation (28) to the opposite, which reflects the symmetry of the particle's motion with respect to the origin.

Equations (28) and (29) can be combined into a single equation valid for all $z \in \mathbb{Z}$ as follows:

$$\partial_z f(z,t) + \mathrm{sgn}(z) 7rp\, 2^{|z|} \partial_t f(z,t) = 0. \tag{30}$$

It can be shown that the second moment of the particle's position in the process described by (30) grows logarithmically with time. Hence, in the continuous limit, the NOS model with even rigidity exhibits sub-diffusive behaviour.

2.4.3 OS Model

The delay times t_{lj} and their probabilities a_{lj} for the case when the elementary lattice length is ζ and the elementary time step is τ can, again, be obtained by replacing z with $N = z/\zeta$ in the expressions derived in the previous section. Hence, for $z > 0$ we have:

$$\begin{cases} t_0 = 0, \\ t_{lj} = 2r(N+j), & 1 \le l \le z, \;\; j \ge l-1, \\ a_0 = q, \\ a_{lj} = C_{N-1}^{l-1} C_j^{l-1} q^N p^{j+1}, & 1 \le l \le z, \;\; j \ge l-1. \end{cases}$$

Note that, as before, in the limit $\zeta \to 0$, N becomes unbounded.

By straightforward computation, we obtain the following formulae for $\langle t_D \rangle$ and $\mathrm{Var}(t_D)$:

$$\begin{aligned} \langle t_D \rangle &= \tau \left(2r\frac{p}{q}N + 1 \right), \\ \mathrm{Var}(t_D) &= 4\tau^2 r^2 \left(\frac{p}{q}N^2 + N\left(\frac{p}{q}\right)^2 \right). \end{aligned}$$

Now, dividing $\langle t_D \rangle$ and $\mathrm{Var}(t_D)$ above by ζ and taking the limit $\zeta \to 0$, $\tau \to 0$ we get:

$$\begin{aligned} \frac{1}{c} &= 2r\frac{p}{q}z \lim_{\zeta\to 0, \tau \to 0} \frac{\tau}{\zeta^2}, \\ \gamma &= 4r^2\frac{p}{q}z^2 \lim_{\zeta\to 0, \tau \to 0} \frac{\tau^2}{\zeta^3}. \end{aligned}$$

For these quantities to stay bounded, both of these limits must be finite. Hence, we require that

$$\lim_{\zeta\to 0, \tau \to 0} \frac{\tau}{\zeta^2} = 1. \tag{31}$$

Under this condition, $\gamma = 0$, and the expression for $1/c$ simplifies to:

$$\frac{1}{c} = 2r\frac{p}{q}z. \tag{32}$$

Substituting $1/c$ given by (32) and $\gamma = 0$ into (25), we obtain the continuous limit of equation (23):

$$\partial_z f(z,t) + 2r\frac{p}{q}z\partial_t f(z,t) = 0. \tag{33}$$

Similarly, the continuous limit of equation (24) reads

$$\partial_z f(z,t) - 2r\frac{q}{p} z \partial_t f(z,t) = 0. \tag{34}$$

The above two equations can be combined into a single equation which is valid for all $z \in \mathbb{Z}$:

$$\partial_z f(z,t) + 2r \left(\frac{p}{q}\right)^{\mathrm{sgn}(z)} |z| \partial_t f(z,t) = 0. \tag{35}$$

In the model described by this equation, the second moment of the particle's position grows linearly with time. Hence, in the continuous limit, the OS model exhibits diffusive behaviour.

Remark: The results obtained in this section agree with the earlier results about the diffusive properties of the one-dimensional WRE models in [10].

2.5 NOS Model and Memory Effect

Up until now we assumed that the scatterers are distributed independently over the lattice vertices. In this section, we explore the effect of dependency between the scatterers on the dynamics of the system. We study a modified version of the NOS model with rigidity one, where the probabilities of forward- and back-scatterers at neighboring vertices $i-1$ and i are related, i.e. the environment of scatterers has memory.

We consider the following distribution of scatterers. Let q_i and $p_i = 1 - q_i$ denote the probabilities of forward- and back- scatterers at vertex i at time 0. Then the vector of probabilities $\vec{P}(i) = (q_i, p_i)$ satisfies the following recurrent relation:

$$\vec{P}(i) = \vec{P}(i-1)\, M, \tag{36}$$

where M is a Markov-type matrix:

$$M = \begin{pmatrix} 1-P & P \\ Q & 1-Q \end{pmatrix}$$

for some $0 \leq P, Q \leq 1$.

The first-visit equation for the modified NOS model still has the form (4), but the coefficients in the r.h.s. of the equation now depend on z, i.e.:

$$f(z+1, t+1) = q_z f(z,t) + p_z f(z, t-2).$$

In order to find the coefficients p_z and q_z, we note that $\vec{P}(z) = \vec{P}(0)M^z$. Employing the standard method for computing M^z, by using the eigenvalues and eigenvectors of M:

$$\begin{aligned} \lambda_1 &= 1, & \vec{v_1} &= (1,1)^T, \\ \lambda_2 &= 1 - P - Q \equiv \lambda, & \vec{v_2} &= (P, -Q)^T, \end{aligned}$$

we find:

$$M^z = I + \frac{1}{P+Q} \begin{pmatrix} -P & P \\ Q & -Q \end{pmatrix} (1 - \lambda^z).$$

Hence,

$$\begin{aligned} q_z &= q_0 + \beta(1 - \lambda^z), \\ p_z &= p_0 - \beta(1 - \lambda^z), \end{aligned}$$

where $\beta = (Q\,p_0 - P\,q_0)(P+Q)^{-1}$.

For a scaled version of the model, where the elementary time step is τ and the elementary lattice length is ζ, we need to replace z in the above expressions with $N = z/\zeta$. The first-visit equation in this case reads:

$$f(z+\zeta, t+\tau) = q_N f(z,t) + p_N f(z, t-2\tau).$$

The average time that takes the particle to propagate from z to $z+\zeta$ and its variance can be found by straightforward computation:

$$\begin{aligned} \langle t_D \rangle &= q_N\,\tau + p_N\,3\tau = \\ &= (1 + 2p_0) - 2\beta + \mathcal{O}\left(\lambda^N\right), \\ \mathrm{Var(t_D)} &= q_N\,\tau^2 + p_N\,(3\tau)^2 - (q_N\,\tau + p_N\,3\tau)^2 = \\ &= 4(p_0 - \beta)(q_0 + \beta) + \mathcal{O}\left(\lambda^N\right), \qquad \text{as } N \to \infty. \end{aligned}$$

Next, we use definition (26) to compute the coefficients $1/c$ and γ in the continuous limit equation (25):

$$\begin{aligned} \frac{1}{c} &= \frac{Q+3P}{Q+P} \lim_{\zeta\to 0,\tau\to 0} \frac{\tau}{\zeta}, \\ \gamma &= \frac{4PQ}{(Q+P)^2} \lim_{\zeta\to 0,\tau\to 0} \frac{\tau^2}{\zeta}. \end{aligned}$$

Since these coefficients must stay bounded as both ζ and τ aproach 0, we require that

$$\lim_{\zeta\to 0,\tau\to 0} \frac{\tau}{\zeta} = 1.$$

Under this condition, $\gamma = 0$ again, and the continuous limit equation reads:

$$\partial_z f(z,t) + \frac{Q+3P}{Q+P} \partial_t f(z,t) = 0,$$

which describes the propagation on the real line with the velocity $(Q+P)/(Q+3P)$. Compare this to the continuous limit equation we obtained earlier for the case of independent scatterers (27). The only difference between the two is the velocity with which the particle propagates. Thus, the dependency between the scatterers at neighboring vertices does not affect the qualitative behaviour of the system, although it may change its quantitative characteristics.

Note that, if $P + Q = 1$, then the model "loses" memory and reduces to the standard NOS model where the forward- and back-scatterers are distributed over the lattice vertices independently with probabilities Q and P respectively. In this case, the propagation speed reduces to $(1+2P)^{-1}$, which agrees with the expression obtained in the section that deals with the NOS model with odd rigidity.

2.6 Multi-Particle NOS Model: Statistical Properties

In this section, we study the statistical properties of the one-dimensional multi-particle NOS model with rigidity one (also known as the one-dimensional FM model) introduced earlier in this chapter. As before, we denote the initial concentration of back-scatterers as p. It is assumed that the particles are distributed uniformly with

density ρ on the lattice, and that initially there are no identical particles, i.e. particles with the same positions and velocities. This is a natural assumption because the NOS model does not provide a mechanism for merging several particles into a super-particle or splitting a particle into several sub-particles. Also, existing particles do not disappear, nor do new particles emerge in the course of evolution.

It is also assumed that the particles do not interact with each other directly. However, collisions of the particles with the scatterers result in changes to the environment, thereby causing indirect, or *asynchronous*, interactions between the particles. Clearly, as long as a particle does not encounter a trace of any other particle, its dynamics is the same as it would be in the case of a single-particle model. It was shown in [41] that, in the absence of other particles, a single particle propagates in one direction with random speed. The direction of propagation is determined by the initial velocity of the particle and the configuration of scatterers at the initial position of the particle and its nearest neighbors. The average speed of propagation $\bar{v}$ depends on the concentration of back-scatterers p; the two quantities are related via $\bar{v} = (1 + 2p)^{-1}$.

In order to completely define the dynamics of the multi-particle model, we need to specify what happens when more than one particle hits the scatterer. There are two approaches. In the first, the scatterer flips whenever it is hit by any number of particles. We refer to the variation of the NOS model with this type of interaction as Model A. The second approach is based on the idea that the particles create a pressure on the scatterer. The pressure is considered balanced when two particles hit the same scatterer at the same time (from the opposite sides), so the scatterer does not flip. It will flip, however, when it is hit by a single particle, and the pressure is no longer balanced. We refer to this variation of the NOS model as Model B.

We investigate the statistical properties of the multi-particle NOS model with both types of interactions, and attempt to answer the following questions:

- Are the particle trajectories bounded or unbounded?

- If the trajectories are unbounded, what does the distribution of particle displacements look like at a given time instant, and how does it change with time?

- How do the model's parameters p and ρ affect the system's behaviour?

2.6.1 Simulation Results

To answer the questions stated above, a number of simulations were performed with different concentrations of back-scatterers p and densities of particles ρ, on a lattice consisting of $L = 10^4$ vertices. For given values of p and ρ, a set of $5/\rho$ independent realizations of each model was created by randomly distributing particles and scatterers with appropriate densities among the vertices of the lattice. Each such realization involved $L\rho$ particles, so the total number of particles involved in each set of realizations with the same values of ρ and p was approximately 5×10^4.

For each realization, we let the system of particles run for 10^6 time steps and recorded the displacements of all particles every 10^4 steps. Periodic boundary conditions were used in both Model A and Model B. However, if a particle crossed the boundary, its displacement was computed as though it had entered a neighboring copy of the original lattice interval. Statistical properties were obtained by considering average quantities, where the averages were taken over all initial configurations of scatterers and particles with given probabilities p and ρ. The Java source code for the simulation program is available by request.

The simulations showed that both models exhibit similar behaviour, so the results stated below apply to both models unless noted otherwise.

In the multi-particle NOS model, the observed distribution of particle displacements was close to Gaussian for any density of particles $\rho \in (0, 2)$ and any concentration of scatterers $p \in [0, 1]$, as demonstrated by the Q-Q plots in Figures 4-5. This distribution exhibited the following properties:

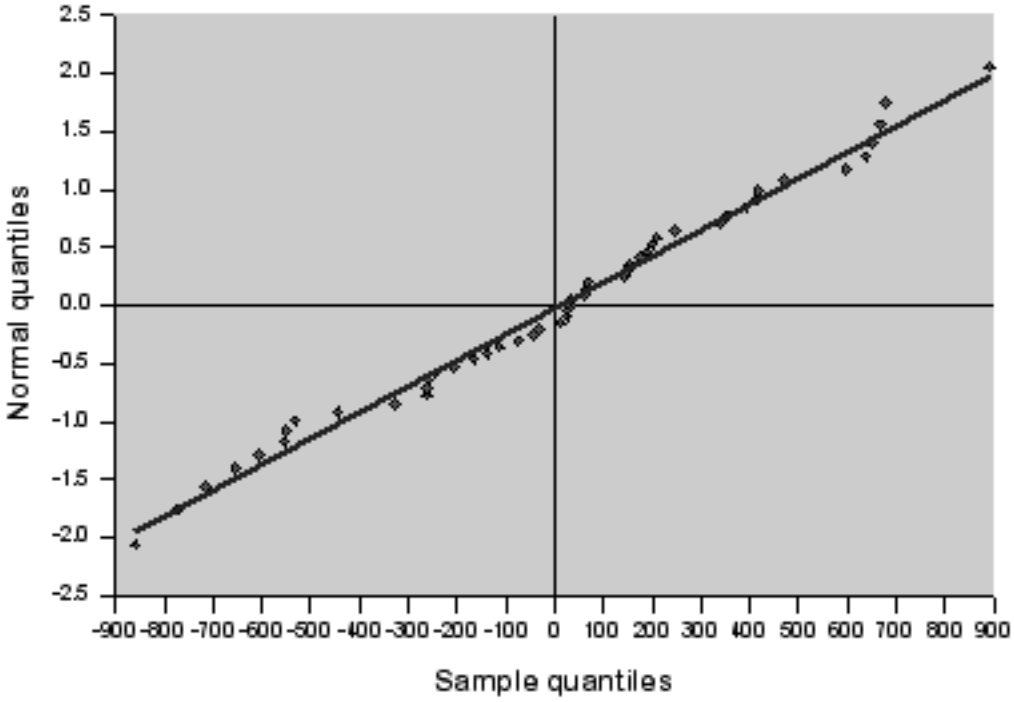

Figure 4: Q-Q plot of sample quantiles of particle displacements in Model A versus the quantiles of a standard normal distribution. Model parameters: $p = 0.5$, $\rho = 0.5$, $t = 10^5$.

- Its mean value fluctuated around zero without any visible pattern (see Figures 6-7). For large concentrations of particles, the 95% significance intervals for almost all observed means included 0, as shown in Figure 7. Since the particles are equally likely to propagate in either direction on $\mathbb{Z}$, it is reasonable to assume that the mean of the distribution is 0 at any time.

- As expected, its variance decreased as the concentration of particles increased. The graphs of mean square displacements versus time for several different concentrations of particles ρ are shown in Figures 8-9. These graphs show that the mean square displacement, and therefore, the variance of the distributions of particle displacements grow linearly with time. The slopes of these lines decrease as the concentration of particles grows. Hence, we can say that the

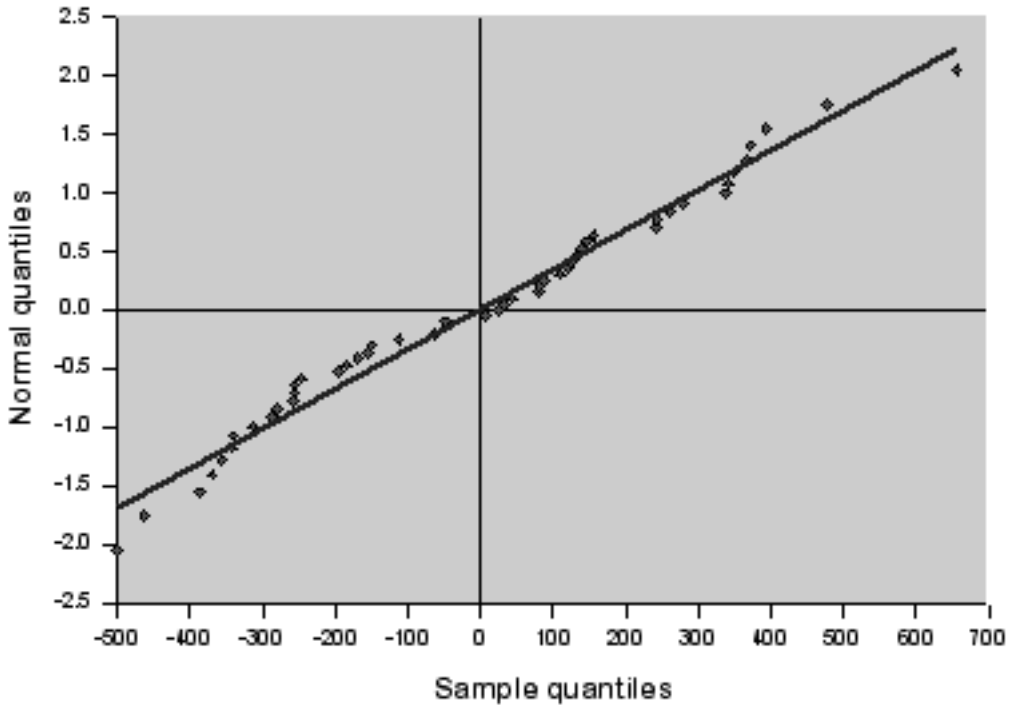

Figure 5: Q-Q plot of sample quantiles of particle displacements in Model B versus the quantiles of a standard normal distribution. Model parameters: $p = 0.5$, $\rho = 0.5$, $t = 10^5$.

particle interactions slow down their respective propagation. Note that the slopes tend to 0 as the concentration of particles approaches 2. In fact, in the extreme case $\rho = 2$, the dynamics of the system becomes completely different from that observed for other values of ρ; this case will be discussed in more detail in the next section.

- The distribution of particle displacements did not exhibit any dependence on the concentration of back-scatterers p. The simulations were performed for three different values of p in the interval [0,1]. A small density of particles ($\rho = 0.1$) was selected to increase the potential impact of the environment on the dynamics of the system. However, the obtained distributions were nearly identical.

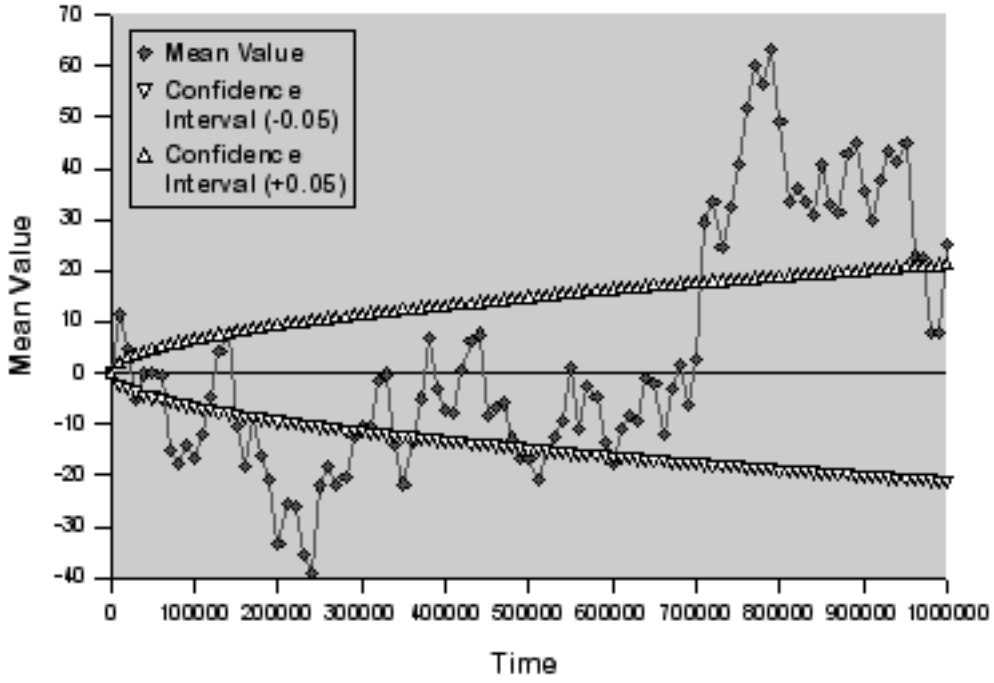

Figure 6: Mean values of the distribution of particle displacements for a small concentration of particles in Model A. Model parameters: $p = 0.5$, $\rho = 0.1$, $t = 10^6$.

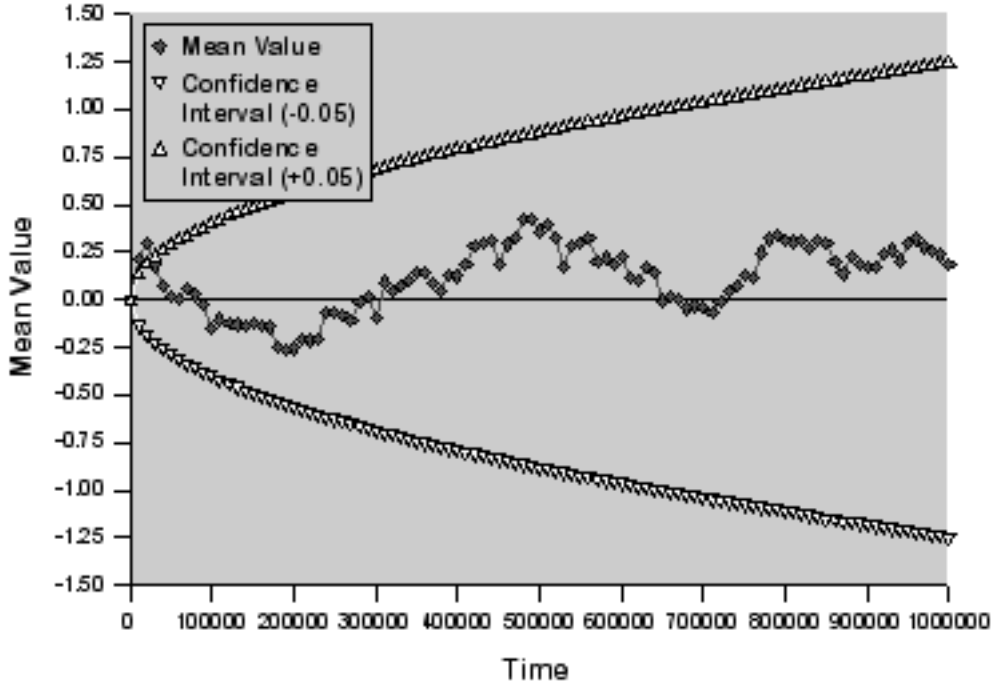

Figure 7: Mean values of the distribution of particle displacements for a large concentration of particles in Model A. Model parameters: $p = 0.5$, $\rho = 1.5$, $t = 10^6$.

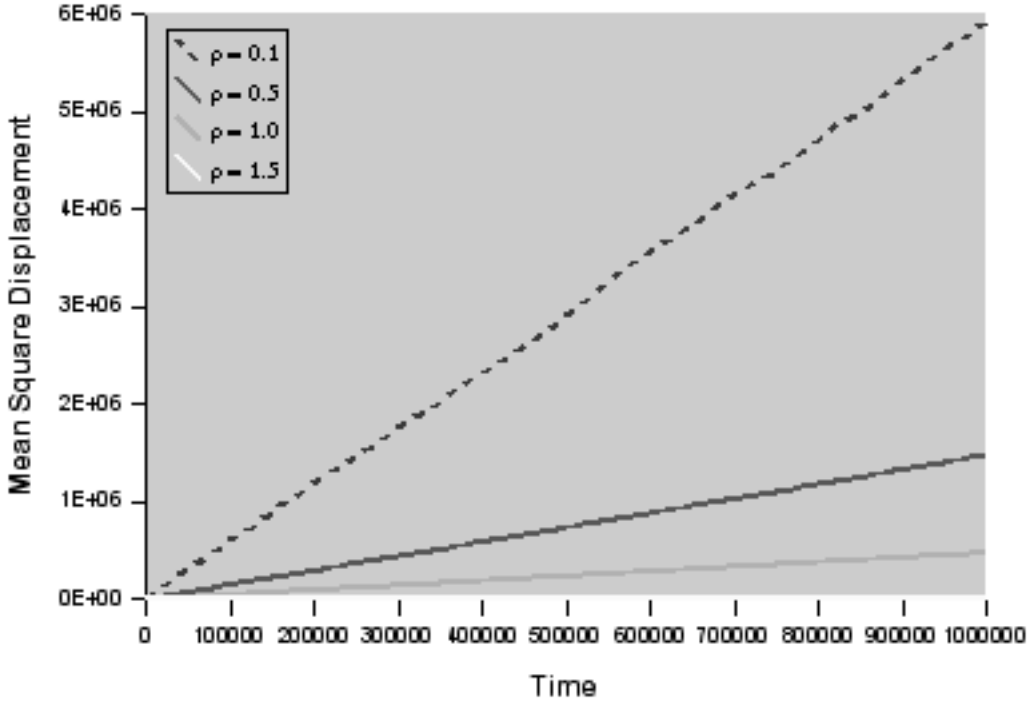

Figure 8: Mean square displacements of particles as a function of time for different concentrations of particles in Model A with $p = 0.5$.

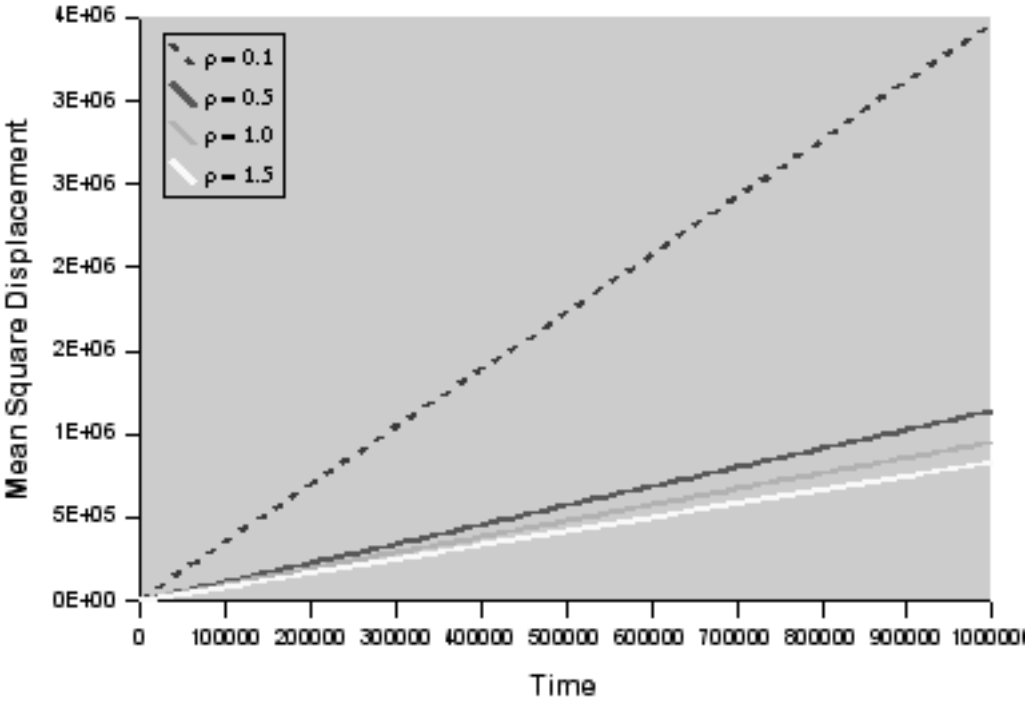

Figure 9: Mean square displacements of particles as a function of time for different concentrations of particles in Model B with $p = 0.5$.

2.6.2 Full Occupancy Case

The case where the lattice is fully occupied by the particles (i.e. $\rho = 2$), exhibits different behaviour and should be considered separately. In fact, this behaviour is similar for both variations of the NOS model and can be completely described analytically.

PROPOSITION 2.1 *In the fully occupied multi-particle NOS model with rigidity 1 the trajectories of all particles are periodic with probability 1.*

Proof: We start with the case of Model B. Since the lattice is fully occupied, and no particles appear or disappear during the system's evolution, every vertex of the lattice hosts 2 particles (with opposite velocities) at any moment of time. Therefore, at each time instant, each scatterer gets hit by exactly two particles and thus, does not flip, according to the interaction rules for this model. This means that the fully occupied Model B is identical to the fixed mirror model (see Chapter I). In this model the environment does not change with time and the trajectory of a single particle is known to be periodic. But, since the environment is fixed, the particles do not "know" about the presence of others, so the trajectories of all particles in the system are periodic. More precisely, each particle bounces between the two closest back-scatterers on each side of its initial position.

Next, we shall prove the proposition for Model A. As in the case of Model B, at each time instant each scatterer gets hit by two particles. In this case, however, the scatterers will flip. Hence, every scatterer on $\mathbb{Z}$ flips every time step.

We denote the initial position of a particle by z and, without loss of generality, assume that its initial velocity is positive: $v = 1$. For the particle to change its velocity, it has to encounter a back-scatterer. This happens if, at $t = 0$, there was either a forward scatterer at position $(z+2k)$ or a back-scatterer at position $z+(2k-1)$ for some $k > 0$. Indeed, it would take exactly $2k$ time steps for the particle to reach the position $(z + 2k)$. During this time, the forward scatterer at this position flips

$(2k-1)$ times, thus becoming a back-scatterer at the time when the particle arrives at this vertex. A similar argument can be used for the back-scatterer scenario. The probability of either event is 1, so with probability 1, the particle changes its direction.

After the particle changes its velocity to the opposite, it retraces the path to its initial position z, and continues moving in the negative direction until it encounters another back-scatterer. The same argument used above for the positive direction can be repeated here to show that this event occurs with probability 1.

The only thing left to show is the periodicity of the particle's motion. This can be achieved by a simple observation that the number of time steps between two successive visits of the particle to the same site is even. Therefore, each scatterer is always in the same state (BS or FS) every time the particle visits it. Hence, from the particle's perspective the environment is fixed, so the particle's motion is periodic, as it was in the case of Model B. This completes the proof of the Proposition.

2.7 Concluding Remarks

As we mentioned in the Introduction, deterministic walks in random environments are generated by two processes: the deterministic motion in the region D_t formed by all vertices visited by the particle to the moment t, and a random process of propagation into the complement $\bar{D}_t$ of this region. In general, this region changes with time. Equation (1) is a general equation that describes the motion of the boundary of this deterministic region. The models under study demonstrate sub-diffusive, diffusive and super-diffusive types of behaviour for the boundary that consists of only two points.

The deterministic character of motion inside region D_t is the reason why continuous limits of the kinetic equations for all of the models explored in this text contain only the propagation term. Indeed, the motion of the particle inside the deterministic region D_t has no fluctuations. Moreover, the fluctuations on the boundary ∂D_t,

which are generated by random distribution of scatterers outside of D_t, are relatively small. This situation should be compared with the biased random walk (see e.g. [33]), whose continuous limit contains a fluctuation term due to the pure randomness of the corresponding model. Biased random walk allows for an appropriate scaling of probabilities of transitions [33], while no such scaling exists for deterministic walks in random environments.

CHAPTER III

LLG WITH ROTATING SCATTERERS

3.1 Introduction

The LLG model studied in this chapter was originally introduced in [50]. It is a modification of the classical one-dimensional Lorentz lattice gas in which the scatterers are freely rotating disks with their centers fixed on a regular triangular lattice. Infinitely many non-interacting point particles move in an array of such scatterers. Although the particles do not interact directly, they exchange energy with each other through the disks by changing the disk's angular velocities. Thus, as with FLLG, analyzing the system with just one moving particle will not give us full understanding of the dynamics of the multi-particle model.

Nevertheless, the one-particle model is interesting by itself as a highly nontrivial infinite-dimensional dynamical system. The first step in studying the time evolution of a dynamical system is to find its simplest solutions. And this is the goal of this study. We consider orbits in which the velocity of the particle is tangential to just one row (or column) of scatterers. In other words, we assume that the array of scatterers is one-dimensional. However, even after all these simplifications are made, the dynamics is still quite complex. We have been able to analyze it completely for only a few values of the model's parameter. It is interesting to note that, for some of these values, the model is equivalent to the deterministic Lorentz lattice gas with flipping scatterers [10],[13],[58]. It is quite remarkable that this seemingly artificial and largely simplified model appears as an exact (albeit special) solution to an extremely complicated model which is currently considered to be one of the most relevant systems to study the transport phenomena.

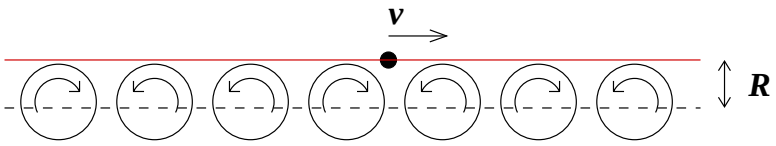

Figure 10: The LLG with rotating scatterers under study. The centers of the scatterers are fixed on a one-dimensional lattice $\mathbb{Z}$. A point particle moves along the line parallel to this lattice and tangential to the disks. No assumptions are being made about the disk's angular velocities, i.e. both the magnitude and the direction are arbitrary.

The results presented in this chapter have been submitted for publication in the Journal of Statistical Physics [15].

We consider a one-dimensional array of freely rotating circular scatterers of radius R with a finite moment of inertia Θ. The centers of the scatterers are fixed on a one-dimensional lattice $\mathbb{Z}$. We consider all possible initial configurations of the scatterers, i.e. all possible configurations of their angular velocities at $t = 0$. A point particle moves along the line parallel to this lattice and tangential to the disks (see Figure 10). The normal component of the particle's velocity is assumed to be 0, so by *velocity* of the particle we mean its tangential component. For an arbitrary initial configuration of scatterers, i.e. when no assumptions are made about their distribution, the system under study becomes completely deterministic. The results obtained in this text describe the possible qualitative behaviours of its orbits. Additional probabilistic assumptions about the initial distribution of angular velocities would allow for quantitative (statistical) description of the ensemble of orbits.

Let v denote the velocity of the particle, and ω the angular velocity of a disk. The collision of the particle with the disk proceeds according to the following rules:

$$\begin{cases} v' = v - \dfrac{2\eta}{(1+\eta)}(v - R\omega) \\ \omega' = \omega + \dfrac{2}{R(1+\eta)}(v - R\omega). \end{cases} \tag{37}$$

Here v' and ω' are the velocity of the particle and the angular velocity of the disk

after the collision; $\eta = \Theta/(mR^2) > 0$ is the only parameter of the model, and can be viewed as the amount of energy transfer between the disk and the particle. It should be noted that this transformation conserves energy and angular momentum [50].

3.2 Exact Solutions

First, note that the dependence on the radius of the disks R in (37) can be eliminated by rewriting the system using disk velocities $w = R\omega$ instead of their angular velocities ω. The equations can be further simplified by introducing a new parameter

$$\kappa = \frac{\eta - 1}{\eta + 1} \in [-1, 1]$$

to replace η in (37). If $t_-(t_+)$ denotes the time instant just before (after) the interaction of the particle with the scatterer, and $t \equiv t_+$, then the system (37) is equivalent to:

$$\begin{cases} v(t+1) = v(t) - (1+\kappa)(v(t) - w(t)) \\ w(t+1) = w(t) + (1-\kappa)(v(t) - w(t)). \end{cases} \tag{38}$$

where time is measured in the number of the particle's collisions with the scatterers. We refer to this discrete time when speaking of time, unless noted otherwise. The qualitative results obtained in this text are valid for both the discrete and the real time, due to Proposition 3.1 below.

Since the dependence on R has been eliminated from these equations, we assume that the radii of disks in Figure 10 are negligibly small, and the particle is moving on the lattice $\mathbb{Z}$.

This system of equations can be completely solved for some values of parameter κ. The following subsections describe these exact solutions. Without loss of generality, we assume that the initial velocity of the particle is positive. We denote as $w_i(t)$ the angular velocity of the disk at position $i \in \mathbb{Z}$ at time t, and $w_i \equiv w_i(0)$. Throughout this chapter, the rotating scatterers with positive angular velocities will be referred to

as right scatterers (RS), and those with negative angular velocities as left scatterers (LS). By *flipping* a scatterer we mean changing its type, i.e. LS $\Leftrightarrow$ RS.

PROPOSITION 3.1 *In the one-particle LLG model (38) with $\kappa \neq -1$, the particle never stops at any vertex for more than one time step.*

Proof: Suppose that the particle stops at time $(t+1)$, e.g. $v(t) \neq 0$ and $v(t+1) = 0$ for some t. Then the first equation of (38) can be solved for $w(t)$, when $\kappa \neq -1$:

$$w(t) = \frac{k}{1+k}\, v(t).$$

Now, we can use this to compute the particle's velocity at the next time instant:

$$\begin{aligned} v(t+2) &= v(t+1) - (1+\kappa)(v(t+1) - w(t+1)) = \\ &= (1+\kappa)w(t+1) = \\ &= (1+\kappa)\left(w(t) + (1-\kappa)(v(t) - w(t))\right) = \\ &= v(t). \end{aligned}$$

Since, by our assumption, $v(t) \neq 0$, the particle will be forced to move. In fact, it will resume its motion in the direction it was moving just before it stopped.

Remark: It will be shown later that, when $\kappa = -1$, the particle propagates with the constant velocity and, therefore, never stops.

Case 1: $\kappa = 0$

When $\kappa = 0$ the system (38) reduces to

$$\begin{cases} v(t+1) = w(t) \\ w(t+1) = v(t), \end{cases}$$

so the particle and the disk simply exchange velocities during the collision. If a particle moving to the right encounters a right scatterer, it passes through it and continues moving in the positive direction without flipping the scatterer. If it hits a left scatterer, however, say at position z, it bounces back to position $(z-1)$. This

position, however, is occupied by a right scatterer (since the particle previously passed through it), so the particle gets reflected back to z. Note that, during the first collision of the particle with the LS at z, the scatterer flips, thus becoming RS. Hence, the second time the particle arrives at z, it passes through the scatterer without changing its direction or flipping it.

Thus, once the particle passes through a scatterer, a *blocking pattern*, similar to the one in LLG models with flipping scatterers (see, e.g. [41]), forms behind it and prevents it from moving in the negative direction for more than one step. This proves the following

PROPOSITION 3.2 *In the one-particle LLG model (38) with $\kappa = 0$, the particle ultimately propagates in one direction. The direction of propagation depends on the configuration of scatterers at the particle's initial position and its nearest neighbors.*

The particle with positive initial velocity ultimately propagates to the left only if $w_0 < 0$ and $w_1 < 0$. For all other combinations of scatterers it propagates to the right.

This behaviour is very similar to that of the one-dimensional NOS model with rigidity one. In fact, when the initial velocities of the disks satisfy $|w_i| = 1$ for all $i \in \mathbb{Z}$, and the disks with positive and negative velocities are distributed over the lattice vertices independently with probabilities q and $p = 1 - q$ respectively, the particle's dynamics in the two models are identical. The average velocity of propagation in this case can be computed directly and is related to the initial density of left scatterers p via:

$$\bar{v} = \frac{1}{1+2p}. \tag{39}$$

Case 2: $\kappa = 1$

In this case the system (38) reduces to

$$\begin{cases} v(t+1) = -v(t) + 2w(t) \\ w(t+1) = w(t), \end{cases} \tag{40}$$

so the angular velocities of the scatterers do not change in the course of evolution: $w_i(t) = w_i$; and the environment is *fixed*. We show that in this scenario there are only two possible regimes of the particle's motion: either the particle propagates in one direction on $\mathbb{Z}$, or its trajectory is periodic. Let $z(t)$ denote the particle's position at time $t \geq 0$.

PROPOSITION 3.3

- *(i) If the initial configuration of scatterers in the one-particle LLG model (38) with $\kappa = 1$, satisfies:*

$$2\sum_{k=1}^{2n}(-1)^{k+1}w_{z(k)} \leq v(0) \leq 2\sum_{k=1}^{2n-1}(-1)^{k+1}w_{z(k)} \text{ for any } n \geq 1, \tag{41}$$

  then, after at most one time step, the particle propagates to the right: $v(t) \geq 0$ for all $t \geq 1$.

- *(ii) If the initial configuration of scatterers satisfies:*

$$2\sum_{k=1}^{2n-1}(-1)^{k+1}w_{z(k)} \leq v(0) \leq 2\sum_{k=1}^{2n}(-1)^{k+1}w_{z(k)} \text{ for any } n \geq 1, \tag{42}$$

  then, after at most one time step, the particle propagates to the left: $v(t) \leq 0$ for all $t \geq 1$.

- *(iii) For any other configuration of scatterers, after a finite number of steps, the particle gets trapped inside a unit interval $[i, i+1]$ for some i.*

Proof: (i)-(ii) We will prove that parts (i)-(ii) of the Proposition provide the necessary and sufficient conditions for the particle's propagation. Indeed, for the particle to propagate to the right after one time step, the following inequality must be satisfied for each $t \geq 1$:

$$\begin{aligned} 0 \leq v(t) &= -v(t-1) + 2w_{z(t)} = \\ &= (-1)^t \left(v(0) + 2\sum_{k=1}^{t}(-1)^k w_{z(k)} \right), \end{aligned} \tag{43}$$

where $\{z(k)\}_{k\geq 0}$ denotes the particle's trajectory. Writing this inequality for $t = 2n$ and $t = 2n - 1$ yields the pair of inequalities (41). The conditions for the particle's propagation to the left can be derived in the same manner by reversing the inequality sign in (43).

(iii) Let us suppose now that conditions (i)-(ii) are not satisfied. Since these are the necessary and sufficient conditions for the particle's propagation, there must exist such t that either $v(k) \geq 0$ for all $1 \leq k \leq t$ and $v(t+1) < 0$, or $v(k) \leq 0$ for all $1 \leq k \leq t$ and $v(t+1) > 0$. Let us assume that the former set of conditions is satisfied (the other case can be handled in the similar manner), and suppose that, at time t, the particle arrives at some position $i > 0$. Then its velocity satisfies the following equations:

$$\begin{aligned} v(t) &= -v(t-1) + 2w_i, \\ v(t+1) &= -v(t) + 2w_{i+1} = v(t-1) + 2(w_{i+1} - w_i). \end{aligned} \tag{44}$$

Since, by our assumption, $v(t-1) > 0$ and $v(t+1) < 0$, the second equation of this sequence implies that the initial configuration must satisfy $w_{i+1} < w_i$.

We use induction to show that the particle will be forever trapped in the interval $[i, i+1]$. It suffices to show that the following inequalities are satisfied for all $k \geq 0$:

$$\begin{aligned} v(t+2k) &> 0. \\ v(t+2k+1) &< 0 \end{aligned} \tag{45}$$

Their validity for $k = 0$ was shown to be a simple consequence of the conditions that constitute case (iii). Let us assume that they are also satisfied for up to $k = n - 1$. This means that during the time interval $[t, t+2n-1]$, the particle was bouncing between positions i and $i+1$. Let us evaluate the velocity of the particle at $t + 2n$, noting that at this time instant it arrives at position i:

$$\begin{aligned} v(t+2n) &= -v(t+2n-1) + 2w_i = \\ &= v(t+2n-2) - 2(w_{i+1} - w_i). \end{aligned}$$

But, as we showed earlier, $w_{i+1} < w_i$, so $v(t+2n) > v(t+2n-2) > 0$. Thus, the direction of the particle's motion changes once again, and it proceeds to position $i+1$. At the subsequent time instant we have

$$\begin{aligned} v(t+2n+1) &= -v(t+2n) + 2w_{i+1} = \\ &= v(t+2n-1) + 2(w_{i+1} - w_i) \\ &< v(t+2n-1) < 0, \end{aligned}$$

which completes our proof by induction. The immediate corollary to inequalities (45) is that the particle turns every time it visits either i or $(i+1)$, thus never leaving the interval $[i, i+1]$. It is interesting to note that the speed of the particle is continually increasing:

$$|v(t+k)| = |v(t)| + 2k(w_i - w_{i+1}), \tag{46}$$

and, therefore, tends to infinity.

Remark: The conditions of part (iii) of Proposition 3.3 are satisfied if, for example, $0 < v(0) < 2w_1$ and the initial concentration of left scatterers is positive. Indeed, the inequalities guarantee that this configuration does not satisfy the conditions of part (ii). Moreover, since the concentration of left scatterers is positive, then, with probability one, the particle will encounter one of them, i.e. $w_{i+1} < 0$ for some i. Then,

$$v(t+1) = -v(t) + 2w_{i+1} < 0,$$

and so, this configuration does not satisfy conditions of part (i) either. Hence, it falls under conditions of part (iii).

Case 3: $\kappa = -1$

For this value of the parameter κ, the system (38) reduces to

$$\begin{cases} v(t+1) = v(t) \\ w(t+1) = 2v(t) - w(t), \end{cases}$$

and the dynamics of the particle becomes trivial. The following Proposition follows immediately from these equations:

PROPOSITION 3.4 *In the one-particle LLG model (38) with $\kappa = -1$, the particle propagates in one direction, with constant speed $v(t) = v(0)$, for any initial configuration of scatterers.*

Case 4: $-1 < \kappa < 0$

For negative values of κ, the system (38) can be rewritten in the form:

$$\begin{cases} v(t+1) = \alpha v(t) + (1-\alpha) w(t) \\ w(t+1) = (1+\alpha) v(t) - \alpha w(t), \end{cases} \tag{47}$$

where $\alpha = |\kappa|$. A simple analysis of signs of the particle's and disk's velocities, before and after the collision, allows us to prove the following:

PROPOSITION 3.5 *The trajectory of the particle in the one-particle LLG model (38) with $\kappa < 0$ is unbounded.*

Proof: Table 3 lists all valid sign combinations for the velocities of the particle and the disk, before and after the collision. It is easy to verify that no other combination satisfies both equations in (47).

Suppose that the trajectory is bounded. Then the particle visits a finite number of vertices on $\mathbb{Z}$ infinitely many times. Let us consider the right-most such vertex and denote it as z^*. This means that the particle must always be scattered to the left at this vertex. But, as Table 3 shows, the particle moving with a positive velocity will turn back at z^* only if it encounters a left scatterer. And not only does the particle turn, it also flips the scatterer: $w(t+1) > 0$. Hence, during the particle's next visit to z^* the velocities of both participants will be positive, and the particle will pass through the scatterer. This contradicts our assumption that z^* was the right-most vertex visited by the particle. Thus, the character of interaction between the particle

Table 3: A list of valid sign combinations for the velocities of the particle and the disk before and after their interaction, when $\kappa < 0$.

$v(t)$	$w(t)$	$v(t+1)$	$w(t+1)$
+	+	+	+
+	+	+	−
+	−	+	+
+	−	−	+
−	+	+	−
−	+	−	−
−	−	−	+
−	−	−	−

and scatterers pushes the particle outside of any finite region, and its trajectory is unbounded.

More can be said about the particle's dynamics, when $\kappa = -1/2$ and the initial velocities of the particle and the disks are the same in magnitude: $|w_j(0)| = |v(0)|$ for all $j \in \mathbb{Z}$. In this case the system (47) further reduces to:

$$\begin{cases} v(t+1) = 1/2v(t) + 1/2w(t) \\ w(t+1) = 3/2v(t) - 1/2w(t), \end{cases} \tag{48}$$

and we can prove the following

PROPOSITION 3.6 *If the initial configuration of scatterers and the particle in the one-particle LLG model (38) with $\kappa = -1/2$, satisfies*

$$|w_j(0)| = |v(0)| \text{ for all } j \in \mathbb{Z}$$

then the particle propagates with the velocity $v(0)$.

Proof: There are only two possibilities to consider: when the velocity of the particle $v(t)$ is the same as or is opposite to the velocity of the scatterer $w(t)$.

If $v(t) = w(t)$ then the particle and the scatterer "ignore" each other:

$$\begin{cases} v(t+1) = v(t) \\ w(t+1) = w(t), \end{cases} \tag{49}$$

and their respective velocities do not change during the collision.

If $v(t) = -w(t)$, then the velocities of the particle and the disk at subsequent moments of time satisfy the following equations:

$$\begin{cases} v(t+1) = 0 \\ w(t+1) = -2w(t), \\ v(t+2) = -w(t) = v(t) \\ w(t+2) = w(t). \end{cases} \tag{50}$$

Thus, after two time steps, the system returns to the state it was in right before the particle's collision with the scatterer. The particle stops immediately after the collision, but continues moving in its original direction after just one time step. Hence, the direction of the particle's motion never changes, and is completely determined by the direction of its initial velocity.

To compute the velocity of propagation, note that it takes one time step for the particle to pass through a right scatterer and two time steps to pass through a left scatterer. However, in real time the second time step is instantaneous since the particle is interacting twice with the same scatterer. Hence, regardless of the type of scatterer encountered by the particle, it takes the same amount of time for the particle to move one lattice step in the direction of propagation. Therefore, the particle propagates with constant speed which is independent on the initial configuration of scatterers and, according to (49)-(50), is equal to $v(0)$.

PROPOSITION 3.7 *If the initial configuration of scatterers and the particle in the one-particle LLG model (38) with $\kappa < 0$, satisfies*

$$sgn\, w_j = sgn\, v(0) \quad \text{for all } j \in \mathbb{Z},$$

then the particle propagates in the direction of its initial velocity.

Proof: If the initial velocities of the disks and the particle are positive (negative), then the r.h.s. of the first equation in (47) is always positive (negative). Hence,

the sign of the particle's velocity never changes in the course of propagation, so the particle propagates in the direction of its initial velocity.

PROPOSITION 3.8 *If the initial configuration of scatterers and the particle in the one-particle LLG model (38) with $\kappa < 0$, satisfies both of the following conditions*

- $v(0) > (1 + 1/\kappa)w_1$ *(respectively* $v(0) < (1 + 1/\kappa)w_1$*)*
- $w_j \geq \kappa w_{j-1}$ *(respectively* $w_j \leq \kappa w_{j-1}$*) for all* $j \in \mathbb{Z}$*,*

then the particle propagates to the right (left).

Proof: The Proposition can be proved by induction. We consider the case of propagation to the right. The first of the two conditions guarantees that the particle passes through the first scatterer it encounters:

$$\begin{aligned} v(1) &= -\kappa v(0) + (1 + \kappa)w_1 = \\ &= -\kappa(v(0) - (1 + 1/\kappa)w_1) > 0. \end{aligned} \tag{51}$$

Assuming that, at time i, it passes through the scatterer located at position i, i.e.:

$$v(i) = -\kappa v(i - 1) + (1 + \kappa)w_i > 0, \tag{52}$$

we evaluate the particle's velocity after its collision with the next scatterer on its path:

$$\begin{aligned} v(i + 1) &= -\kappa v(i) + (1 + \kappa)w_{i+1} = \\ &= \kappa^2 v(i - 1) + (1 + \kappa)(w_{i+1} - \kappa w_i). \end{aligned} \tag{53}$$

Since $w_{i+1} > \kappa w_i$, the r.h.s of this equation is positive, so the velocity of the particle stays positive after the collision. Thus, the particle keeps moving in the positive direction.

The case of the particle's propagation to the left can be considered by reversing the signs in the inequalities above.

Case 5: $\kappa > 0$

No rigorous statements concerning the particle's dynamics for positive κ can be proven as of yet. Results of simulations of this system suggest that the particle's trajectory is unbounded. At this point, however, this is only a conjecture.

We can, however, prove a statement analogous to Proposition 3.8 for $\kappa > 0$, by applying the same technique and reusing equations (51)-(53) without any changes:

PROPOSITION 3.9 *If the initial configuration of scatterers and the particle in the one-particle LLG model (38) with $\kappa > 0$, satisfies both of the following conditions*

- $v(0) < (1 + 1/\kappa)w_1$ *(respectively* $v(0) > (1 + 1/\kappa)w_1$*)*
- $w_j \geq \kappa w_{j-1}$ *(respectively* $w_j \leq \kappa w_{j-1}$*)* for all $j \in \mathbb{Z}$,

then the particle propagates to the right (left).

3.3 Concluding Remarks

The two-dimensional LLG model with rotating scatterers introduced in [50] is an extremely complex infinitely dimensional dynamical system. In this text, we have found some of its simplest orbits.

We have found the simplest orbits of the Lorentz gas with rotating scatterers and demonstrated that, in some cases, its dynamics is similar to the dynamics of the one-dimensional flipping Lorentz lattice gas [10]. We also need to point out one notable difference. All of the results in this text were obtained by introducing discrete time into the model, the technique often used when studying LLG. In classical LLG cellular automata (i.e SLLG, FLLG, WRE) the real-time and the discrete-time dynamics are equivalent. But this is only partially the case for LLG with rotating scatterers. Qualitatively, the dynamics of the particle is the same in both the real time and the discrete time due to Proposition 3.1. Its quantitative characteristics, however, may

be different. Indeed, the speed $|v_d|$ of the particle with respect to the discrete time is always bounded: $v_d \in \{0, 1\}$. Moreover, its average speed satisfies $1/2 \leq \langle |v_d| \rangle \leq 1$ (see Proposition 3.1). On the other hand, it is possible to find a configuration of scatterers, in which the particle's speed with respect to *real time* tends to 0 or infinity (see e.g. equation (46) in the proof of Proposition 3.3) as time increases.

On the other hand, it would be interesting to compare the dynamics of the one-particle Lorentz gas with rotating scatterers on the triangular lattice [50] with the dynamics of classical LLG on this lattice [12]. One of the natural questions would be: which types of scattering rules on the latter can mimic the dynamics of the former?

CHAPTER IV

TWO-DIMENSIONAL LLG WITH FLIPPING SCATTERERS

4.1 Introduction

This chapter deals with the dynamics of two-dimensional flipping Lorentz lattice gases on regular and random lattices. As before, G denotes the lattice (regular or random) in the Euclidean space $\mathbb{R}^2$, and S denotes the set of all scatterers on G. For each model we choose a subset $\hat{S} \subseteq S$ of scatterers which may appear at the lattice vertices, and distribute these scatterers among all vertices according to some translationally invariant probability distribution.

A general definition of an LLG model with flipping scatterers is best given using terminology borrowed from the theory of Turing machines [8]. This also illustrates the potential application of Lorentz lattice gases in theoretical computer science. Let us assume that, at each vertex $g \in G$, there is a tape $Q(g)$ satisfying the following two conditions:

- $Q(g)$ is partitioned into an infinite number of cells $q_i(g)$, $i = 1, 2, \ldots$;
- Some scattering rule $s_i(g) \in \hat{S}$ is "coded" into each cell $q_i(g)$, $i = 1, 2, \ldots$.

The dynamics of flipping LLG on the lattice G is defined as follows [8]: a particle travels with the unit speed along the edges of G. If it comes to vertex $g \in G$ for the i-th time then:

1. The particle gets scattered at g according to the local scattering rule $s_i(g)$, and

2. $Q(g)$ shifts to the left by one position.

It has been proven in [41] that, in the LLG model with flipping rotators on the regular triangular lattice, the particle always propagates in a strip. In this text we look at the reorganization of the medium that takes place after the passage of the particle, and investigate the interaction properties of propagating particles.

We demonstrate that on random (Poisson and vectorizable) triangular lattices a particle either propagates in an infinite random strip, or is trapped inside a closed random strip. It is our conjecture that the probability of unbounded orbits is positive. However, the way to prove this result remains unclear. We also demonstrate that the probability of bounded (periodic) orbits is positive. Until now, periodic orbits have been observed numerically for the Poisson lattice [63], but not for the vectorizable lattice.

We also show that the propagation observed in the FR model on the triangular lattice is not possible in the analogous rotator models on the regular square and hexagonal lattices.

This chapter is composed of the results that have been previously published in [12] and [13].

4.2 Description of Models

In this text we discuss LLG models with flipping scatterers on various types of lattices, both regular and random. The lattices include the square ($\mathbb{Z}^2$), triangular ($\mathbb{T}^2$) and hexagonal ($\mathbb{H}^2$) lattices as well as the Delaunay random lattice ($\mathbb{D}^2$).

The Delaunay random lattice ([22],[34],[52]) is defined as the dual lattice to the Voronoi tessellation of the plane (see Figure 11). For a given set of points, the Voronoi tessellation is constructed as follows: for each point of the set, we define a cell associated with it as a region of the plane which is nearer to this point than to any other point of the set [38]. Any two such cells sharing an edge are considered

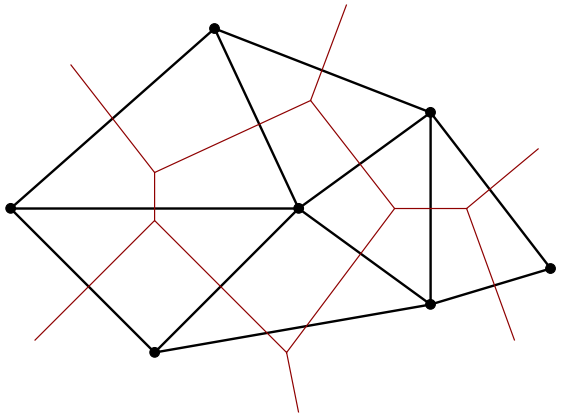

Figure 11: Duality between the Voronoi tessellation of the plane (thin red lines) and the Delaunay random lattice (thick black lines)

neighbors. (In the literature they are referred to as contiguous.) By connecting every two points associated with the neighboring cells by a line segment, we obtain a triangulation of the plane called a Delaunay random lattice. One of the most important properties of this lattice is the following (see e.g. [53]):

Property 4.1 *The circle circumscribed around any triangular cell of the Delaunay random lattice does not contain any lattice points inside.*

We consider two known variations of the Delaunay random lattice: a Poisson random lattice (PRL) and a vectorizable random lattice (VRL), which differ by the initial distribution of the lattice points. The first is obtained by distributing the points randomly and uniformly over the infinite plane. To construct the second lattice, the plane is covered with a regular square lattice and then the points are distributed randomly and homogeneously inside each square in such a way that each square contains only one point. By connecting the points using the procedure described above, we obtain the two variations of the Delaunay random lattice. More details can be found in e.g. [63].

In all models, we assume that the lattice is fully occupied by right (R) or left (L) rotators which rotate the velocity vector of a particle arriving at the vertex by

the largest possible angle to the right or to the left respectively. In the case of the regular square lattice, this angle is equal to $\pi/2$. For the regular triangular and hexagonal lattices, it is equal to $2\pi/3$ and $\pi/3$ respectively (see Figure 12). Initially, the scatterers are placed at the vertices independently with probabilities P_R and $P_L = 1 - P_R$. A single particle travels along the edges of the lattice, with unit speed, in all possible directions and gets scattered at the lattice vertices. A scatterer flips ($L \Leftrightarrow R$) each time it is hit by the particle.

4.3 FLLG on Regular Lattices

4.3.1 FR model on $\mathbb{T}^2$.

First we need to introduce several definitions. We define a *strip* as a region of $\mathbb{T}^2$ bounded by two adjacent parallel lines, both oriented along one of the lattice axes.

We say that a particle propagates in one direction in a strip S if, after some finite time, its motion is confined to S, and any vertex in the strip is visited no more than a fixed number of times. This behaviour can be naturally viewed as a glider in random medium.

It has been shown that the FR model on the regular triangular lattice $\mathbb{T}^2$ demonstrates quite unexpected behaviour:

THEOREM 4.1 [41] *For any initial distribution of rotators on fully-occupied $\mathbb{T}^2$, a moving particle propagates in one direction in a strip on the lattice. Both the strip and the direction of propagation depend on the initial configuration of rotators at the initial position of the particle and its nearest neighbors.*

This result is due to the existence of a mechanism that produces a *blocking pattern* based on a zigzag path of length four. On the regular triangular lattice, the blocking pattern consists of two pairs of parallel velocity vectors at four consecutive time steps (see Figure 13). It uniquely defines the propagation strip as well as the direction of

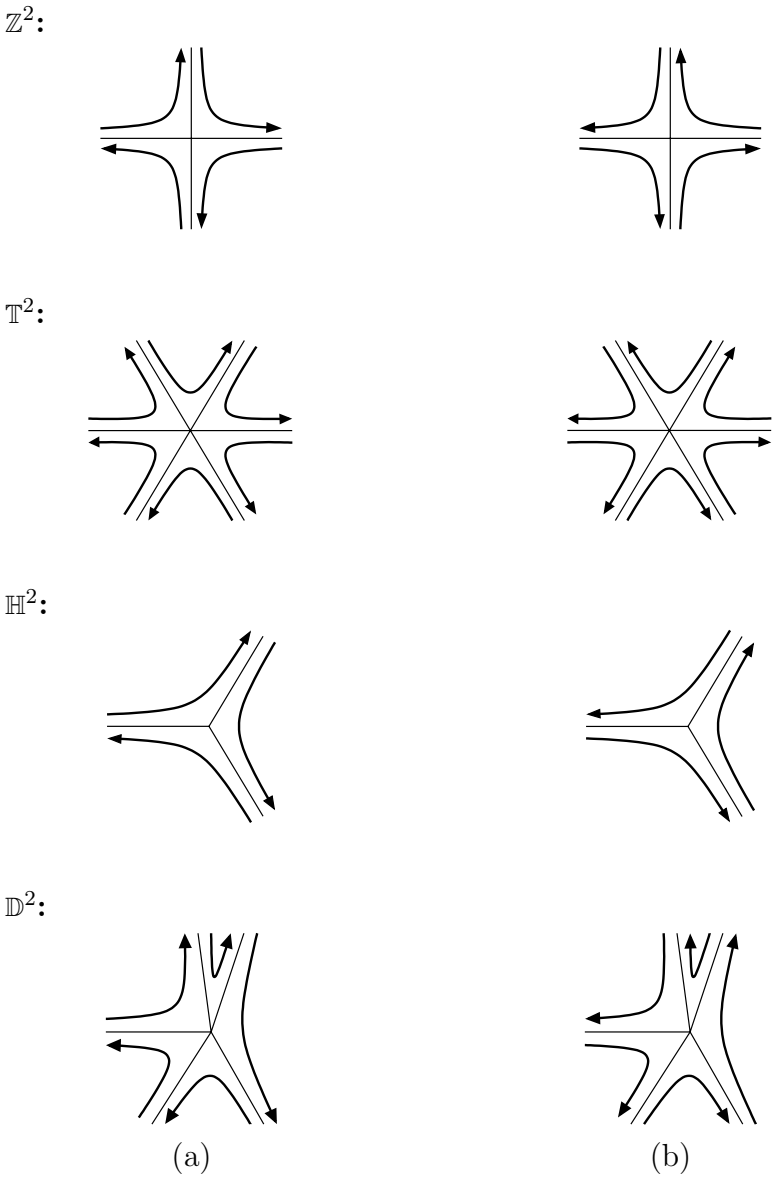

Figure 12: Left (a) and right (b) rotators on the square ($\mathbb{Z}^2$), triangular ($\mathbb{T}^2$), hexagonal ($\mathbb{H}^2$) and Delaunay ($\mathbb{D}^2$) lattices. If we enumerate the edges meeting at a vertex 0 through $n-1$ clockwise, then a general local scattering rule at this vertex is given by the function $\phi : \{0, \ldots, n-1\} \to \{0, \ldots, n-1\}$. This means that a particle approaching a vertex along edge i will leave that vertex along edge $\phi(i)$. In these notations, a right rotator corresponds to the function $R(i) = i - 1 (\mathrm{mod}\ n)$ and a left rotator to $L(i) = i + 1 (\mathrm{mod}\ n)$.

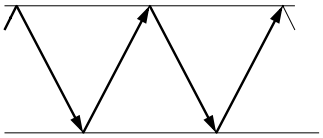

Figure 13: A blocking pattern on a regular triangular lattice. Arrows indicate the successive velocity vectors of the particle.

propagation. Such a pattern always appears after a finite number of steps (which do not exceed eleven [41]) and serves two purposes: first, it keeps the orbit of the particle strictly confined to the strip, and second, it prevents the particle from ever accessing the region of the strip lying on the opposite side of the blocking pattern. Once the particle visits a new site in the strip, the pattern shifts along the edge of the strip in the direction of propagation, thus forcing the particle to continue moving forward.

Every time the particle visits a new site it will, depending on the state of the scatterer at this site, either a) continue moving onto the next site in the direction of propagation, or b) turn back and make an additional six steps before visiting the next site along the strip. We refer to the sites which exhibit outcome a) as *forwarding* sites, and outcome b) as *bouncing* sites. For instance, if a particle propagates from left to right in a horizontal strip, then the sites with R-rotators on the "top" boundary of the strip and those with L-rotators on the "bottom" boundary are forwarding sites, whereas the rest are bouncing sites.

Note that the passage of the particle through a forwarding site results in the flipping of the scatterer at *that* site (see Figure 14.a)), while its passage through a bouncing site flips the scatterer at the vertex located three steps back along the zigzag path from the bouncing site (see Figure 14.b)). No other changes are made to the configuration of scatterers. In both cases the site being passed by the particle is left in the bouncing state. This observation leads to the following statement which has recently been formulated in [4]:

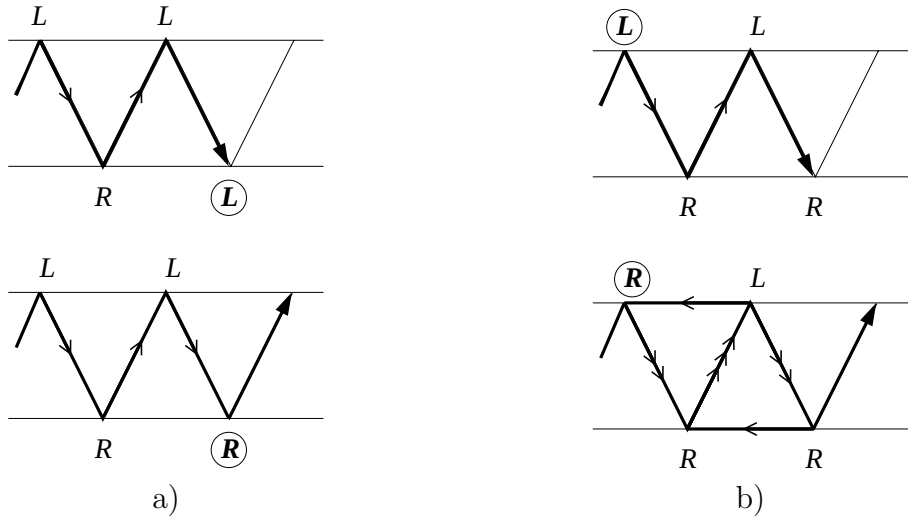

Figure 14: Reorganization of the medium after the passage of a particle in the case of a) forwarding site; b) bouncing site. Arrows indicate successive velocity vectors of the particle. The number of arrows on each edge corresponds to the number of times the particle traveled along that edge.

PROPOSITION 4.1 *The passage of a particle results in a reorganization of the medium in such a way that the initial configuration of scatterers on the strip shifts three steps back along the zigzag path contained in the strip.*

Proof: As noted above, the passage of the particle through a site leaves it in the bouncing state. However, it may become forwarding later, if at $t = 0$, the site located three steps ahead of it along the zigzag path is bouncing. Hence, the passage of the particle results in the reorganization of the medium that can be summarized as follows: the final configuration of forwarding-bouncing sites is exactly opposite to the configuration that can be obtained by shifting the initial configuration along the zigzag path of length three in the direction opposite to the direction of propagation.

Since the endpoints of such a zigzag path belong to the opposite boundaries of the strip, the roles of forwarding and bouncing sites for them are reversed. Hence, if the "head" of a zigzag path was occupied by a certain type scatterer before the particle's first visit to it, then after the particle passes through it, the scatterer of the same

type reappears at the "tail" of this zigzag path. Since this is true for any scatterer, the entire configuration shifts along.

4.3.1.1 FLLG with infinitely many particles

Next, we look at the flipping rotators model on $\mathbb{T}^2$ with infinitely many particles. Note that, as long as a particle does not encounter a trace of any other particle, its dynamics is the same as it would be in the case of a single particle model. Hence, the interactions between the particles are the most interesting and distinguishing feature of multi-particle models.

As in the case of the one-dimensional NOS model, we assume that particles with the same velocity vectors cannot occupy the same vertex. If two particles arrive at the same vertex of the lattice at the same time, they simply pass through each other. We also assume the following multi-particle collision policy: a rotator always flips regardless of how many particles hit it.

We will illustrate some aspects of glider transformations upon their collisions. For this purpose we examine the propagation of particles in the same strip.

Definition 4.1 *The interaction zone of a propagating particle is defined as a region formed by all vertices of the propagation strip located within two lattice unit lengths of the particle position.*

PROPOSITION 4.2 *Suppose that two particles propagate in the same direction in a strip on $\mathbb{T}^2$. If they appear within each other's interaction zone, then after several time steps they will be scattered into new propagation strips.*

Proof: Without loss of generality, we may assume that the particles propagate to the right in a horizontal strip. It is sufficient to consider two possibilities.

If the particles enter each other's interaction zones and, at the time of entering, they lie on the same boundary of the propagation strip, then according to Figure

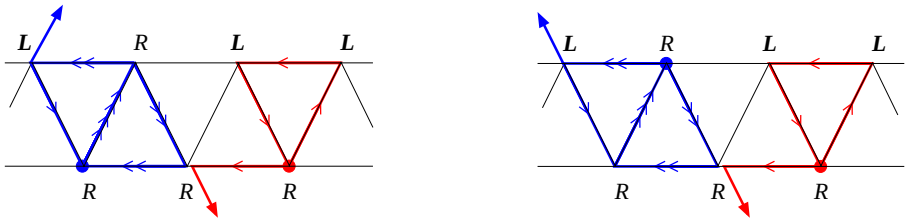

a) b)

Figure 15: Propagation of two particles in the same direction in a strip. If the particles enter each other's interaction zone, after several steps they will be scattered into new propagation strips. Part a) corresponds to the case when the particles enter each other's interaction zones through the same boundary of the strip, and b) to the case when they enter through the opposite boundaries. Arrows indicate successive velocity vectors of the particles. The number of arrows on each edge indicate the number of times the particle traveled along that edge.

15.a), one of the particles leaves the strip after five time steps and the other - after eleven steps. Afterwards both particles continue propagation in their new strips.

If, at the time of entering each other's interaction zones, the particles lie on the opposite boundaries of the propagation strip, then one of the particles leaves the strip after five time steps whereas the other leaves it after twelve steps (see Figure 15.b)). After scattering, both particles continue propagation in their new strips.

We now consider the case when two particles propagate in the same strip but in the opposite directions.

PROPOSITION 4.3 *Suppose that two particles propagate in the opposite directions in a strip on* $\mathbb{T}^2$*. Then, after passing through each other, they will continue their propagation in the original strip in their respective directions.*

Proof: It is sufficient to consider two cases: when the particles pass each other on an edge, and when they "meet" at a vertex.

In the first case the particles, in fact, *do not see* each other (see Figure 16.a)). In the second case, however, they do meet each other several times, but after four time steps they continue propagation in their initial directions (see Figure 16.b)).

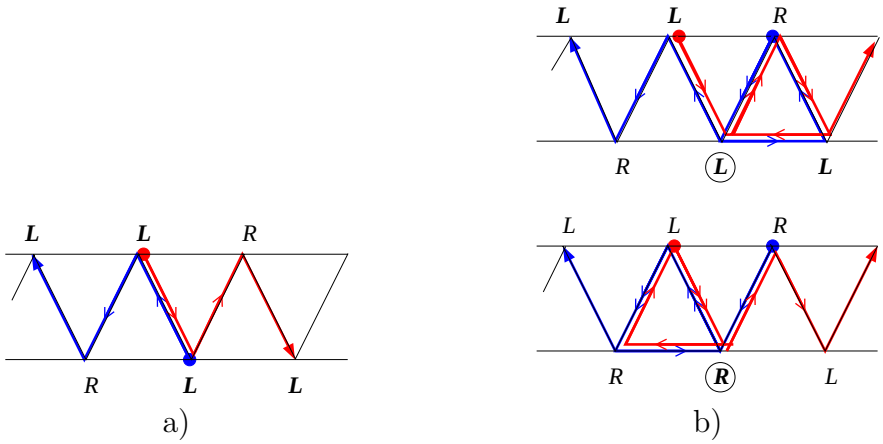

Figure 16: Propagation of two particles in the opposite directions in a strip. After the "interaction", the particles will continue propagation in the same strip in their initial directions. Part a) corresponds to the case when the particles pass each other on an edge, and b) to the case when they meet at a vertex. Arrows indicate successive velocity vectors of the particles. The number of arrows on each edge indicate the number of times the particle traveled along that edge.

Proposition 4.2 shows that, if two or more particles collide (perhaps through the environment), then they can be scattered into new propagation strips. Thus, effective scattering is possible in the multi-particle FR model on $\mathbb{T}^2$. Therefore, generally, particles do not pass through each other like solitons.

4.3.2 FR model on $\mathbb{Z}^2$.

Next, we show that the propagation of the particle in a strip is a feature of triangular lattices. The square and hexagonal FLLG models do not possess this property.

PROPOSITION 4.4 *For almost all configurations of rotators in the FR model on $\mathbb{Z}^2$, a moving particle does not propagate in a strip.*

Proof: Assume, on the contrary, that a particle propagates in some strip S on $\mathbb{Z}^2$. Without loss of generality, we may assume that the direction of propagation has a positive horizontal projection (the case of a strictly vertical strip can be considered by interchanging the horizontal direction with the vertical in the argument below).

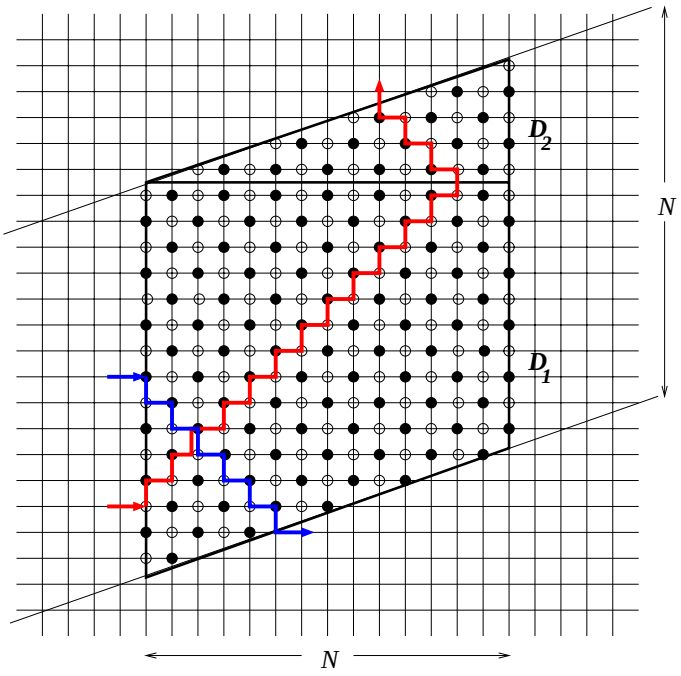

Figure 17: Configuration of scatterers in the region $D = D_1 \cup D_2$ of $\mathbb{Z}^2$ which pushes a propagating particle outside of the strip. Bold lines indicate the trajectories of particles arriving at the left boundary of D. Filled circles denote R rotators, empty circles denote L rotators.

Let N be the height of strip S, measured as the maximum number of vertices lying on any vertical line between the strip boundaries.

Now, let us consider the region D formed by all vertices of S located between two parallel vertical lines lying at a distance N from each other (see Figure 17).

In this region we choose the following configuration of scatterers. First, we fill D with alternating R and L rotators. Then, in the subset $D_2 \subset D$ lying above the horizontal line that passes through the top left corner of D and not including the line itself, we flip the rotators so that all left rotators are now replaced with right rotators, and vice versa. The resulting configuration is shown in Figure 17. By D_1 we denote the complement of D_2 in D. Observe that card $D \leq N^2 < \infty$, therefore, the probability of any configuration of scatterers in D is positive.

By our assumption, the particle propagates in S. Let us decompose S into non-intersecting regions of width N. The configurations of scatterers in these regions are independent and, by our observation above, any configuration inside any of these regions has positive probability. Hence, in the course of propagation, the particle will encounter the configuration shown in Figure 17, with probability one. Now, let us take a look at what happens when the particle arrives at the left boundary of D. If it arrives at a vertex with the R-rotator, then the configuration of rotators in D_1 forces it to move along a "right-down" staircase until it eventually leaves the strip. On the other hand, if the particle arrives at a vertex with the L-rotator, then at first, it is forced to travel along a "right-up" staircase until it leaves D_1 and arrives at the southern boundary of D_2. Here, the direction of the particle's motion changes, and it starts traveling along a "left-up" staircase until it eventually leaves the strip. Both types of trajectories are shown in Figure 17.

This shows that, in the course of propagation, with probability one, the particle will encounter a configuration of rotators which pushes it outside of the strip. This contradiction proves the Proposition.

4.3.3 FR model on $\mathbb{H}^2$.

A statement similar to Proposition 4.4 can be proved for the FR model on the regular hexagonal lattice $\mathbb{H}^2$:

PROPOSITION 4.5 *For almost all configurations of rotators in the FR model on $\mathbb{H}^2$, a moving particle does not propagate in a strip.*

Proof: The proof of this result repeats the proof of Proposition 4.4 above. The configuration of rotators that pushes a particle outside of the strip on $\mathbb{H}^2$, is shown in Figure 18.

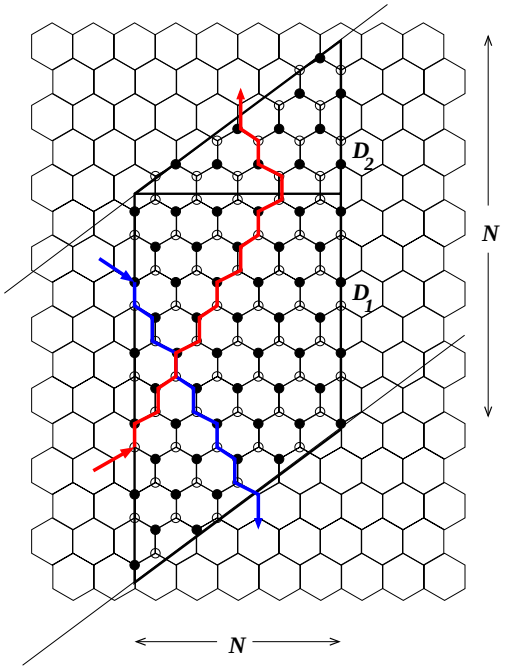

Figure 18: Configuration of scatterers in the region $D = D_1 \cup D_2$ of $\mathbb{H}^2$ which pushes a propagating particle outside of the strip. Bold lines indicate the trajectories of particles arriving at the left boundary of D. Filled circles denote R rotators, empty circles denote L rotators.

4.4 Localization and Propagation in Random Triangular Lattices

Next, we consider the motion of a particle on the Delaunay random lattice $\mathbb{D}^2$, fully occupied by right and left rotators which rotate the velocity vector of a particle arriving at a vertex by the largest possible angle, either to the right or to the left. A rotator flips every time it is hit by a particle. We will see that the behavior of the FR model on $\mathbb{D}^2$ is both similar to and different from that on $\mathbb{T}^2$.

4.4.1 Propagation

First, we show that the FR model on the Delaunay random lattice behaves, to some extent, as it would on the regular triangular lattice. We define a strip on $\mathbb{D}^2$ in a manner similar to the case of $\mathbb{T}^2$. However, the definition introduced earlier needs to

be modified, to reflect the irregular nature of the Delaunay random lattice.

Definition 4.2 *We define a strip on $\mathbb{D}^2$ as a region of the lattice which is formed by all the vertices that a particle visits while performing a zigzag motion on $\mathbb{D}^2$ (i.e. rotating at each step by the largest possible angle to the left or to the right in alternating order).*

The definition of propagation, however, stays the same: we say that a particle propagates in a strip on $\mathbb{D}^2$ if its motion is confined to a strip, and each vertex in this strip is visited no more than a fixed number of times (unless the strip is bounded).

Then the following analogue of Theorem 4.1 can be proved for the FR model on the Delaunay random lattice.

PROPOSITION 4.6 *For any initial distribution of rotators on the fully-occupied $\mathbb{D}^2$, a moving particle always propagates in one direction in a strip on the lattice. Both the strip and the direction of propagation depend on the initial configuration of rotators at the initial position of the particle and its nearest neighbors.*

The proof of Proposition 4.6 repeats that of the identical result for the regular triangular lattice [41], stated earlier as Theorem 4.1. The blocking pattern appearing on the Delaunay random lattice looks like a distorted version of that shown in Figure 13, due to the irregularity of the lattice. The proof of the result in [41] was based entirely on the triangularity of the lattice and did not require the lattice to be regular. An example of a *propagation strip* is shown in Figure 19.

4.4.2 Localization

Let us recall that a propagation strip on the regular triangular lattice is bounded by two parallel lines, therefore no closed trajectories can be found in the fully-occupied FR model on $\mathbb{T}^2$. In Proposition 4.7 below, we show that this is not the case for the Delaunay random lattices. In fact, the randomness of the lattice can cause localization

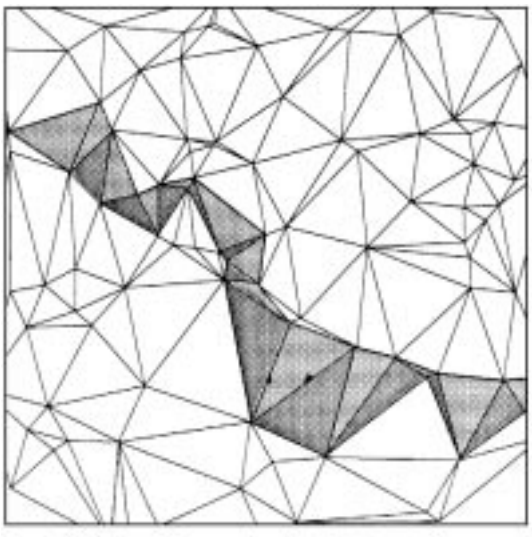

Figure 19: ([41], Figure 1) An example of a propagation strip (shaded area) on the Delaunay random lattice where the particle arriving at a vertex is deflected over the largest possible angle, either to the right or to the left, depending on the R or L nature of the scatterer. Arrows indicate particle displacements.

of orbits in the corresponding FR model. Before we proceed with the proof, however, let us make a few observations:

1) According to Proposition 4.6, the trajectory of a particle is confined to a strip. Therefore, periodic motion should be confined to some bounded, closed strip, i.e. a strip whose boundaries are closed contours on $\mathbb{D}^2$. In what follows, we refer to such a strip as a periodic strip. Examples of such *periodic strips* are shown in Figures 21-24 later in this chapter. It should be noted that the inner and outer boundaries of a periodic strip have equal lengths. Hence, we can define the length of a periodic strip to be equal to the length of either of its boundaries.

2) A particle will never arrive at a periodic strip nor will it leave it. Therefore, the trajectory of a particle placed at the origin is periodic only if the origin belongs to some periodic strip.

3) Due to the nature of the Delaunay random lattice, the length of a closed contour on the lattice is bounded from below by 3. We refer to a strip of length three as a

minimal periodic strip, and the orbit confined to this strip as a minimal periodic orbit.

PROPOSITION 4.7 *The probability of closed trajectories in the FR model on the Delaunay random lattice (PRL or VRL) is positive.*

4.4.2.1 Poisson Random Lattice

Let G be a Poisson random lattice. To prove Proposition 4.7, we will show that the probability of a minimal periodic trajectory on G is positive.

Let C be any triangular cell on G with vertices a_1, a_2 and a_3 . We will show that, with positive probability, the boundary of this cell is the inner boundary of a minimal strip.

The proof requires some additional constructions. Through each vertex a_i, $i = 1, 2, 3$, we draw a line l_i parallel to the segment $a_{i-1}a_{i+1}$ (the index i is understood in the modulo 3 sense). Since these lines are parallel to the sides of cell C, they can not be parallel to each other. For each $i = 1, 2, 3$ we denote the point of intersection of l_{i-1} and l_{i+1} by b_i (see Figure 20).

Finally we denote as D_1, D_2 and D_3 the regions bounded by these lines, as shown in the Figure. Each D_i has a non-zero measure. Hence, with probability one, they contain infinitely many lattice points. Notice also that pairwise intersections of D_i's are empty, therefore the distributions of lattice points inside regions D_i, $i = 1, 2, 3$, are independent.

Inside each D_i we choose a lattice point d_i that gives rise to the circle O_i^d, passing through the points d_i, a_{i-1} and a_{i+1}, of the smallest radius. Note that for each i, the radius of O_i^d is finite. With probability one, each d_i lies in the interior of D_i, so the points a_i, d_{i-1} and d_{i+1} do not lie on the same line, and the circle O_i^a passing through them has a finite radius.

Let us recall that the Delaunay random lattices satisfy Property 4.1 stated above.

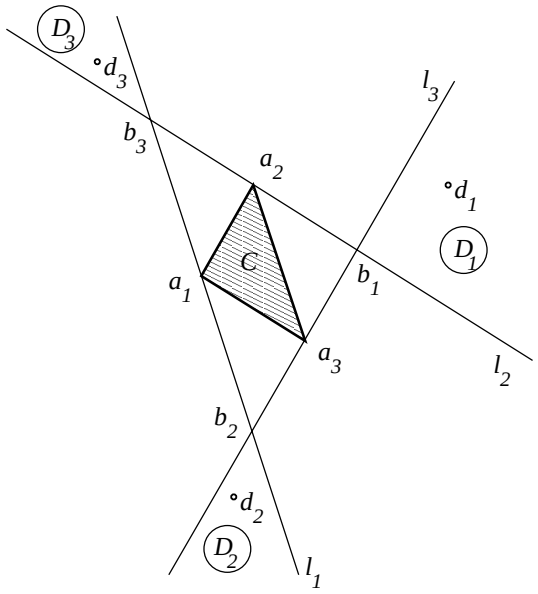

Figure 20: Construction of a minimal periodic strip on PRL in the proof of Proposition 4.7.

Hence, the following statements are equivalent:

- The contour $a_1a_2a_3$ is an inner boundary of a periodic strip;
- The coordination number of each site a_i, $i = 1, 2, 3$, is four;
- The region formed by the union of six circles

$$\left\{\bigcup_{i=1}^{3} O_i^a\right\} \bigcup \left\{\bigcup_{i=1}^{3} O_i^d\right\}$$

  does not contain any lattice points except a_i and d_i, $i = 1, 2, 3$.

The probability of the last event is positive since each of the six circles has a finite radius, and the distribution of the points is uniform over the plane. This proves that the probability that the contour $a_1a_2a_3$ is the inner boundary of a strip is positive.

Since *any* triangular cell, with positive probability, gives rise to a periodic strip, then so do any of the cells that have a vertex at the origin. Hence, with positive probability, the origin belongs to a periodic strip, and a particle placed at the origin has a minimal periodic trajectory.

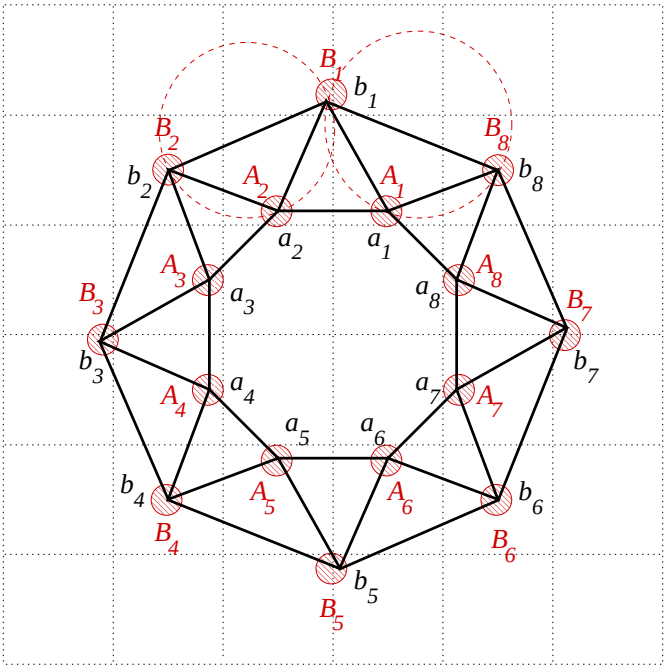

Figure 21: A periodic strip of an even length on VRL. Vertices a_i and b_i, $i = 1, \ldots, 8$, are arbitrary points in the disks A_i and B_i, $i = 1, \ldots, 8$ respectively. Dotted lines indicate the edges of the reference lattice. A circle circumscribed around any cell of the strip must not enclose an "empty" square of the reference lattice. The circles shown here indicate the biggest possible circles arising for the chosen set of vertices.

4.4.2.2 Vectorizable Random Lattice

Let G be a vectorizable random lattice. Since the construction of VRL imposes restrictions on the distribution of vertices on the plane, the argument we used for the PRL case will not work (it is not even clear whether it is possible to construct a periodic strip of length three on VRL).

Nevertheless, we can prove that the contours, which are the inner boundaries of periodic strips, have positive probability. Let us choose eight disks A_i $i = 1, \ldots, 8$ of a sufficiently small radius r as shown in Figure 21. Here, the radii of the disks are chosen to be the same for the sake of simplicity. In principle, they can be different, but they must be small enough for the argument below to hold true. Rigorous analysis of their bounds is beyond the scope of this proof. It suffices to know that all the

radii are positive. If, for each i, r_i denotes the maximum possible radius of A_i, then $r = min_i(r_i)$. Now, inside each disk A_i we pick a point a_i and consider a contour $A = a_1 \dots a_8$. Note that since $r > 0$, the probability that G contains such a contour is positive. Next, let us choose eight disks B_i of the same radius r, as shown in Figure 21. Again, the radii are chosen to be the same, and equal to the radius of the disks A_i, just for the sake of convenience, but neither of those conditions is essential for the construction.

Claim *Any contour $A = a_1 \dots a_8$ with $a_i \in A_i$, $i = 1, \dots, 8$, constructed as above, and contour $B = b_1 \dots b_8$ where $b_i \in B_i$, $i = 1, \dots, 8$, together form a strip, with positive probability. This strip has A as its inner boundary and B as its outer boundary.*

Proof: To prove this Claim, let us notice that by Property 4.1, A and B together form a strip iff, for every i, both the circle passing through a_i, b_i and a_{i+1}, and the circle passing through a_i, b_i and b_{i-1}, do not contain any other lattice points. This event has a positive probability if the circles do not enclose an entire square of the reference lattice that does not contain a_i or b_i for some i. It is easy to see from Figure 21 that, for any choice of the points a_i and b_i from the disks A_i and B_i respectively, all of the mentioned circles satisfy this condition (two sample circles arising from our choice of a_i and b_i, $i = 1, \dots, 8$, are shown in Figure 21 for verification). This concludes the proof of this Claim.

Corollary *Any contour $A = a_1 \dots a_8$ constructed as above is, with positive probability, an inner boundary of a periodic strip.*

Longer contours of any even length greater than 8 can be constructed by adding pairs of segments to the contour in Figure 21 either vertically or horizontally. The same proof can be repeated for contours of any odd length as well (see Figure 22).

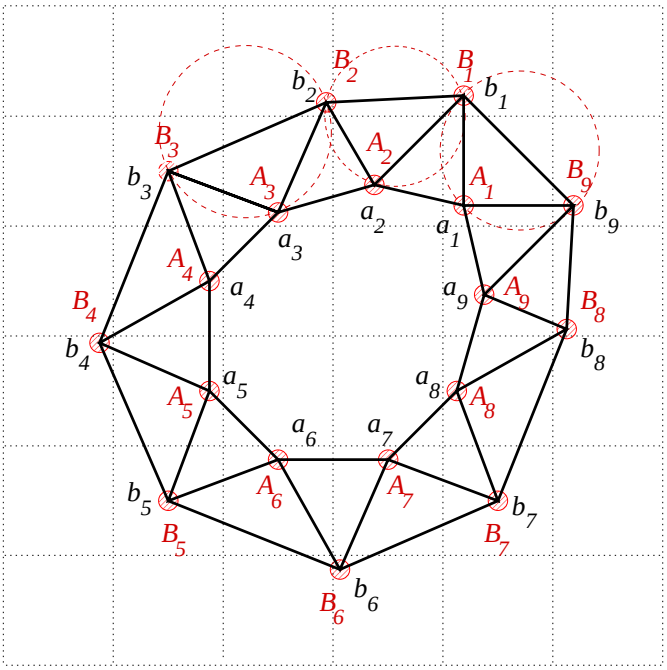

Figure 22: A periodic strip of an odd length on a VRL. Here, we followed the notations used in Figure 21.

Now, combining the Corollary and the fact that the probability of contour A is positive, we conclude that the probability of a periodic strip on a VRL is positive. This concludes the proof of Proposition 4.7 for the case of a VRL.

Remark: Although Proposition 4.7 demonstrates that the probability of bounded trajectories is positive, it does not answer the question whether it is equal to or strictly less than one. Our conjecture is that it is strictly less than one and, therefore, the probability of unbounded trajectories is positive.

4.4.3 Period of the Periodic Motion

According to Proposition 4.1, the configuration of scatterers shifts along the strip with the passage of a particle. Hence, the period of the particle's motion in a periodic strip may involve more than one circuit, or passage of the strip. To illustrate this, let us choose a periodic strip of length 8 (see Figure 23), and trace the position of a scatterer originally placed at the origin a_1, with each circuit (see Table 4).

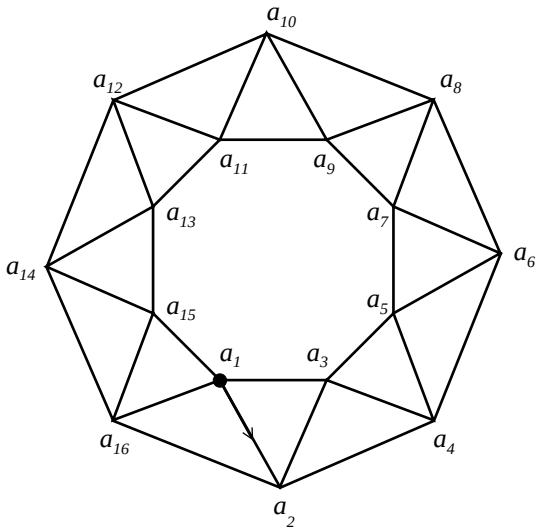

Figure 23: An example of a periodic strip on the Delaunay random lattice. The dot and the arrow indicate the initial position and velocity vector of a particle propagating in this strip.

Table 4: The positions of a scatterer initially placed at a_1, after each passage of the periodic strip shown in Figure 23 by a particle.

Circuit	Position
1	a_{14} then a_{11}
2	a_8
3	a_5
4	a_2
5	a_{15} then a_{12}
6	a_9
7	a_6
8	a_3
9	a_{16} then a_{13}
10	a_{10}
11	a_7
12	a_4
13	a_1

We see that during circuits 1,5 and 9 the scatterer gets shifted twice: first, at the beginning of the circuit to one of the last three positions on the strip and then, again, at the end of the circuit upon passing those positions. This suggests, that for a periodic strip of length n, the period of the particle motion may involve as many as $(2n-3)$ circuits. This observation allows us to find the upper and the lower bounds on the period of the periodic motion.

PROPOSITION 4.8 *The period T of the particle's motion in a strip of length n on $\mathbb{D}^2$ satisfies*

$$8n \leq T \leq 8n(2n-3).$$

Proof: To compute the largest possible period of the particle's motion in a strip of length n, we consider its motion in such a strip after the periodic regime has been established. We enumerate the vertices of this strip a_1 through a_{2n} in the same way as we did in Figure 23 for the previous example, and suppose that, at $t=0$, the particle approaches the scatterer at a_1. According to Proposition 4.1, once the particle passes through a_1, the scatterer shifts three steps back along the strip. Hence, the particle and the scatterer will meet again at position a_{2n-2} and, subsequently, at positions $a_{i(2n-3)+1}$, $i = 2,3,\ldots,N$, where $N(2n-3) = 0 \,(\mathrm{mod}\, 2n)$ and the vertex index is understood in modulo $2n$ sense. Similarly, the entire configuration of scatterers in the block $a_1 \ldots a_{2n-3}$ shifts back along the strip to positions $a_{2n-2} \ldots a_{2n-6}$ and, subsequently, to $a_{i(2n-3)+1} \ldots a_{(i+1)(2n-3)}$, $i = 2,3,\ldots,N$. The motion of the particle will have the largest period when $2n$ and 3 are relatively prime numbers. In this case, $N = 2n$ and the particle will pass $2n$ blocks of $(2n-3)$ scatterers, or, equivalently, make $(2n-3)$ passages of the entire strip before the configuration returns to its initial state.

Now, let us consider the particle's passage through two consecutive blocks of scatterers. Suppose that the first block contained α scatterers in the bouncing state,

or *bouncers*, and $\beta = (2n-3) - \alpha$ scatterers in the forwarding state, or *forwarders*. The configuration of scatterers in the second block is the result of the passage of the particle through the first block. Hence, the configuration of forwarders-bouncers in the former is exactly opposite to that in the latter (see the proof of Proposition 4.1). Since it takes one time step to pass through the forwarding site and seven time steps to pass through the bouncing site, then the time it takes the particle to pass two consecutive blocks of scatterers is given by:

$$T_2 = (7\alpha + \beta) + (7\beta + \alpha) = 8(2n-3),$$

and so, the maximum time required to bring the entire configuration back to its original state is:

$$T_{max} = 8n(2n-3).$$

Note that the period of the particle's motion will be smaller than this upper bound if the initial configuration of scatterers is periodic or when the length of the strip is a multiple of 3.

The smallest possible period of the particle's motion corresponds to the case when the configuration of scatterers at $t = 0$ is periodic with period 3, and the length of the strip n is a multiple of 3. Then, a single passage of the particle through the strip brings the configuration back to its initial state. The periodicity of the initial configuration implies that the same sequence of three scatterers is repeated in the strip $(2n-3)/3$ times. The particle's passage through the first $(2n-3)$ sites of the strip shifts their configuration to $a_{2n-2} \ldots a_{2n-6}$, and its passage through the last three sites shifts the corresponding scatterers again to $a_{2n-5} \ldots a_{2n-3}$.

Let us consider the particle's passage through any two consecutive triangular blocks except the first $(a_1 a_2 a_3)$ and the last $(a_{2n-2} a_{2n-1} a_{2n})$. There are $(2n-6)/3$ such blocks in the strip. The configurations of scatterers in the two consecutive blocks are identical, while the forwarding-bouncing configurations are exactly opposite.

The configuration in the last triangular block $a_{2n-2}a_{2n-1}a_{2n}$ is the result of the passage of $a_1a_2a_3$ by the particle, so their scatterer configurations are also identical, and bouncing-forwarding configurations are opposite. Thus, exactly half of the scatterers the particle encounters during its passage through the strip are bouncers, and half are forwarders. So, the time it takes the particle to return to its initial position a_1 is given by

$$T_{min} = 7n + n = 8n.$$

Remark: The period of the particle's motion is always an even number. Indeed, let α and $\beta = 2n - \alpha$ denote the number of bouncers and forwarders in the strip respectively. Then, the time it takes the particle to complete a single passage is given by $7\alpha + \beta = 2n + 6\alpha$, which is an even number. Since the number of passages of the strip involved in one period cannot be fractional, the period of the motion is always even.

4.4.4 Necessary condition for periodic orbits

Let us assume that there exists a closed (periodic) orbit. We will find a necessary condition for the existence of such an orbit. According to Proposition 4.6 above, this orbit is confined to a closed strip. We denote the inner boundary of this strip as S_{in} and the outer boundary as S_{out}.

PROPOSITION 4.9 *Let Ω be the region of a random lattice contained inside the boundary S_{in} of a periodic strip, including the boundary itself. Then the average coordination number c for this region satisfies the inequality:*

$$4 \leq c < 6.$$

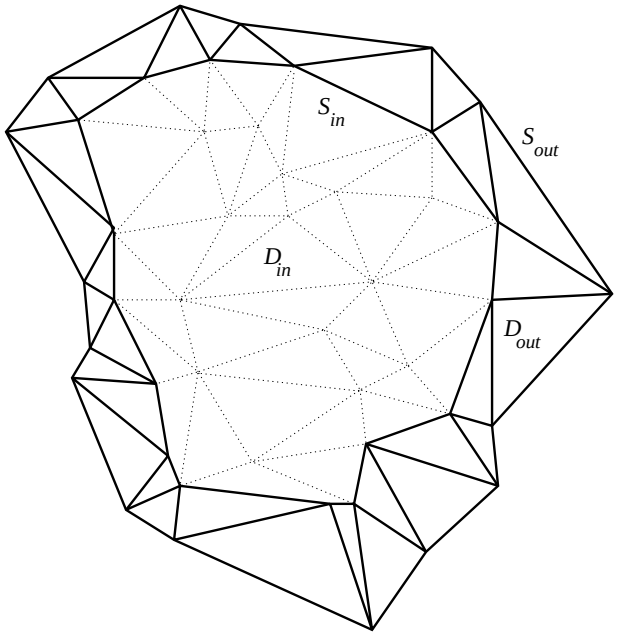

Figure 24: The region $\Omega = D_{in} \cup S_{in}$ in Proposition 4.9. Dotted lines indicate the strip enclosing Ω.

Proof: First, we introduce some notations. We denote the region contained strictly inside S_{in} as D_{in}, and the region strictly outside S_{in} as D_{out}. Also, let $\Omega = D_{in} \cup S_{in}$ (see Figure 24) and Ω^c be its complement in $\mathbb{R}^2$.

To compute the average coordination number, we find the total number T of edges originating at all vertices in Ω and divide it by the total number of these vertices. Let N_S be the number of vertices on S_{in} and N_D be the number of vertices in D_{in}. It is easy to see that, of all edges originating from a vertex of the strip, exactly four are contained in the strip itself. More precisely, two of these edges lie on the boundary and two lie strictly inside the strip. Therefore, each vertex that belongs to S_{in} has exactly two edges in D_{out} and two edges on S_{in} (see Figure 24).

We split the process of computing T into three steps:

Step 1: the number of edges in D_{out}.

Note that only edges originating at the vertices of S_{in} can lie in D_{out}. Moreover, each of the N_S vertices of S_{in} has exactly two edges in D_{out}. Hence, the total number

of edges in D_{out} is equal to $t_1 = 2N_S$.

Step 2: the number of edges on S_{in}.

Similarly, only the N_S boundary vertices have edges lying on S_{in}, and each of these vertices has exactly two such edges. Hence, the total number of boundary edges is equal to $t_2 = 2N_S$.

Step 3: the number of edges in D_{in}.

Let us consider a planar graph H which consists of the triangulated region Ω and an additional face Ω^c. Let t_3 denote the number of edges lying strictly inside D_{in}. Also, let V, F and E denote the total number of vertices, faces and edges in H respectively. Then,

$$E = t_3 + N_S, \;\; V = N_S + N_D, \;\; \text{and} \;\; F = \frac{2t_3 + N_S}{3} + 1.$$

Substituting these values into the Euler's formula $V - E + F = 2$, and solving for t_3 yields:

$$t_3 = N_S + 3(N_D - 1).$$

Now, the sum of the coordination numbers of all vertices in Ω is given by (note that each edge in D_{in} must be counted twice, once for each vertex it connects to):

$$\begin{aligned} T &= t_1 + t_2 + 2t_3 = \\ &= 4N_S + 2N_S + 6(N_D - 1) = \\ &= 6(N_S + N_D - 1) \end{aligned}$$

Finally, to compute the average coordination number, we divide this by the total number of vertices $N = N_S + N_D$:

$$c = \frac{6(N_S + N_D - 1)}{N_S + N_D} = 6\left(1 - \frac{1}{N}\right).$$

As a corollary to this formula, we find that $c < 6$ for any number N. Moreover c is an increasing function of N. Therefore, its minimum is attained when N assumes the least possible value $N_{min} = 3$ (for the case of a minimal periodic strip where $N_D = 0$, $N_S = 3$), and hence is equal to 4. This concludes the proof of Proposition 4.9.

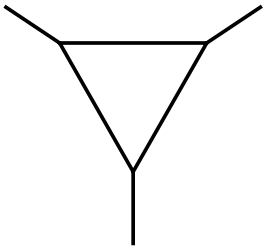

Figure 25: The triangular cell pattern appearing infinitely many times on the random lattices under study (see Property 4.2).

4.5 Rotators with Rigidity One on General Random Lattices

In this section, we study the dynamics of the FR model on random lattices of a more general type. We show that the orbit of a particle moving on an arbitrary (not triangular) random lattice is bounded with probability one, provided that the lattice has the following natural properties:

Property 4.2 *The configuration shown in Figure 25, i.e. a triangular cell, with each of its vertices sharing an edge with exactly three other lattice vertices, appears infinitely many times on the lattice.*

Property 4.3 *With probability one, an unbounded trajectory enters any fixed finite configuration infinitely many times.*

Property 4.2 seems to be a general property for any random lattice of a generic type where the cells are allowed to be polygons with any number of nodes. Property 4.3 holds if, for instance, a distribution of vertices on a random lattice is translationally invariant.

PROPOSITION 4.10 *In the FR model on a lattice satisfying Properties 4.2 and 4.3 above, the trajectory of a particle is bounded with probability one.*

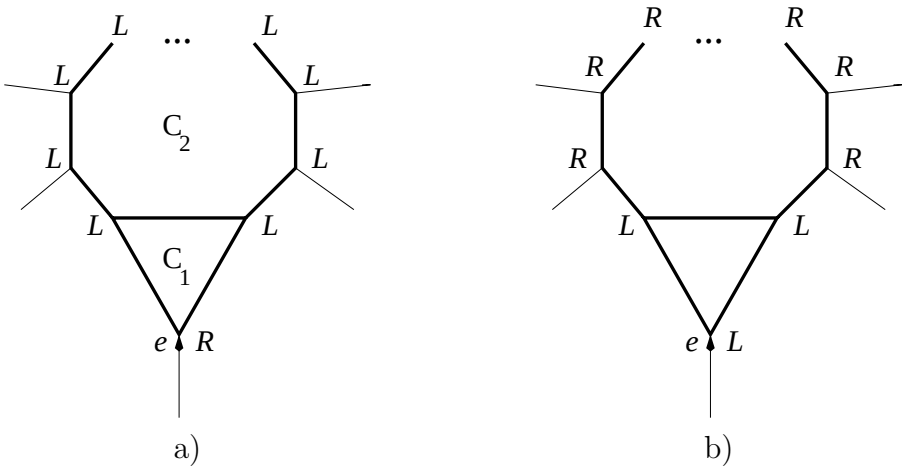

Figure 26: Two states of a reflector. Each time a particle enters configuration a) (b)) through the vertex marked as e (the velocity vector of a particle entering the cluster is indicated by the arrow) it gets "reflected" and the configuration of the cluster switches to b) (a)). The next visit of a particle to this cluster brings it to its initial configuration a) (b)).

Proof: The proof of Proposition 4.10 is based on the existence of so-called *reflectors*, i.e. clusters formed by lattice vertices with the following property: if a particle enters the cluster via a certain vertex, it will exit it, after a finite number of steps, via the same vertex with the opposite velocity (see e.g. [20]).

To give an example of such a cluster, let us consider the triangular cell C_1 as specified by Property 4.2, and an adjacent cell C_2. Now, let us suppose that all vertices of C_2 are occupied by left rotators L, and the remaining vertex of C_1 by a right rotator R, as shown in Figure 26.a). Then it is easy to see that this configuration acts as a reflector. Indeed, if a particle enters the cluster through the vertex marked as e, it will first travel counterclockwise along the boundary of C_1 and return back to e. Then it will travel along the boundary of $C_1 \cup C_2$. After returning to e again, the particle will exit the cluster. Notice that this procedure does not bring the configuration of scatterers to its original state, but instead leaves it in the state shown in Figure 26.b). However, the cluster will return to its original configuration the next time the particle enters this cluster and gets reflected. Notice that the probability of such a reflector

on the lattice satisfying Properties 4.2-4.3 is positive and equal to ${P_L}^n P_R$, where n is the number of vertices in C_2.

Now, let us consider the motion of a single particle on a lattice satisfying Properties 4.2-4.3. Unless its trajectory is bounded, it will encounter infinitely many triangular cells, and hence infinitely many reflectors. Since the environment changes after the passage of the particle, we consider only the first visit of the particle to a reflector. Note also that reflectors may intersect. Hence, if the particle visits a vertex that belongs to more than one reflector, we count it as a visit to all of the reflectors in the intersection. Under this restriction we can assume the reflectors to be independent.

To prove Proposition 4.10, let us assume that the trajectory of a particle is unbounded. Then, as explained above, it will encounter infinitely many independent reflectors. However, each reflector consists of finitely many vertices. Furthermore, the positions and the orientations of reflectors with respect to each other are independent. Therefore, with probability one, the particle will enter one of these reflectors through its entrance point e and be "reflected".

After exiting the reflector, due to the time reversibility of the FR model, the particle will retrace its path to the origin and continue its motion. We can repeat the above argument to conclude that, with probability one, it will enter another reflector through its entrance point e, and be reflected back to the origin again. After that the motion of the particle becomes periodic, with the particle going back and forth between the two reflectors. This yields a contradiction to our assumption. Hence, the trajectory of a particle is bounded with probability one.

4.6 Concluding Remarks

In this text we not only restricted ourselves by the choice of only four lattices, $\mathbb{Z}^2$, $\mathbb{T}^2$, $\mathbb{H}^2$ and $\mathbb{D}^2$, but also imposed the following rules on our models:

- The lattice vertices can be occupied by only two types of local scattering rules.

However, there exist K^K local scattering rules on a lattice with the coordination number K.

- Each vertex of a lattice is occupied by a scatterer. Note that the absence of a scatterer at a vertex is equivalent to the "straight ahead" local scattering rule at that vertex.

However, one can define LLG on any regular or random lattices [23]. Bunimovich and Troubetzkoy studied a variety of LLG models, and proved a number of theorems about the boundedness of the particle's trajectories. Cohen, Kong and Wang analyzed many of these models numerically and studied their diffusive properties. Some of these results were summarized in Tables 1 and 2. For the references to the original publications see the text of Chapter I.

Computer experiments [51] have demonstrated that different types of gliders may exist in the same LLG. It would be interesting to investigate the features of the information transmission in collisions of similar and different gliders.

REFERENCES

[1] Boghosian, B. M., "Lattice gases and cellular automata," *Future Gen. Comp. Sys.*, vol. 16, no. 2-3, pp. 171–185, 1999. Also available at http://arxiv.org/comp-gas/9905001.

[2] Boghosian, B. M. and Coveney, P. V., "A particulate basis for an immiscible lattice-gas model," *Comp. Phys. Comm.*, vol. 129, pp. 46–55, 2000. Also available at http://arxiv.org/cond-mat/9911340.

[3] Boghosian, B. M., Coveney, P. V., and Emerton, A. N., "A lattice-gas model of microemulsions," *Proc. Royal Soc. A*, vol. 452, pp. 1221–1250, 1996. Also available at http://arxiv.org/comp-gas/9507001.

[4] Boon, J. P., "How fast does Langton's ant move?," *J. Stat. Phys.*, vol. 102, pp. 355–360, 2001. Also available at http://arxiv.org/cond-mat/0004331.

[5] Boon, J. P., Grosfils, P., and Lutsko, J. F., "Propagation-dispersion equation," *J. Stat. Phys.*, to appear. Preliminary version is available at http://arxiv.org/cond-mat/0108420.

[6] Bowden, K., ed., *Special issue on general physical systems and the emergence of physical structure from information theory, Int. J. Gen. Syst.*, vol. 27, 1998.

[7] Bradley, R., "Exact θ point and exponents for polymer chains on an oriented two-dimensional lattice," *Phys. Rev. A*, vol. 39, no. 7, pp. 3738–3740, 1989.

[8] Bunimovich, L. A., "Many-dimensional Lorentz cellular automata and Turing machines," *Int. J. Bif. Chaos*, vol. 6, pp. 1127–1136, 1996.

[9] Bunimovich, L. A., "On localization of vorticity in Lorentz gattice gases," *J. Stat. Phys.*, vol. 87, no. 1-2, pp. 449–457, 1997.

[10] Bunimovich, L. A., "Walks in rigid environments," *Physica A*, vol. 279, pp. 169–179, 2000.

[11] Bunimovich, L. A., "Walks in rigid environments: Symmetry and dynamics," *Asterisque*, 2003.

[12] Bunimovich, L. A. and Khlabystova, M. A., "Localization and propagation in random lattices," *J. Stat. Phys.*, vol. 104, pp. 1155–1171, 2001.

[13] Bunimovich, L. A. and Khlabystova, M. A., "Lorentz lattice gases and many-dimensional Turing machines," in *Collision-Based Computing* (Adamatzky, A., ed.), pp. 443–468, Springer-Verlag: London, 2002.

[14] Bunimovich, L. A. and Khlabystova, M. A., "Walks in rigid environments: Continuous limits," *J. Stat. Phys.*, vol. 108, pp. 905–925, 2002.

[15] Bunimovich, L. A. and Khlabystova, M. A., "Lorentz lattice gases with rotating scatterers: Exact solutions," *J. Stat. Phys.*, to appear.

[16] Bunimovich, L. A. and Sinai, Y. G., "Statistical properties of Lorentz gas with periodic configuration of scatterers," *Comm. Math. Phys.*, vol. 78, pp. 479–497, 1981.

[17] Bunimovich, L. A., Sinai, Y. G., and Chernov, N. I., "Statistical properties of two-dimensional hyperbolic billiards," *Russ. Math. Surv.*, vol. 46, no. 4, pp. 47–106, 1991.

[18] Bunimovich, L. A. and Troubetzkoy, S. E., "Recurrence properties of Lorentz lattice gas cellular automata," *J. Stat. Phys.*, vol. 67, pp. 289–302, 1992.

[19] Bunimovich, L. A. and Troubetzkoy, S. E., "Topological properties of flipping Lorentz lattice gas models," *J. Stat. Phys.*, vol. 72, pp. 297–307, 1993.

[20] Bunimovich, L. A. and Troubetzkoy, S. E., "Rotators, periodicity and absence of diffusion in cyclic cellular automata," *J. Stat. Phys.*, vol. 74, pp. 1–10, 1994.

[21] Chernov, N. I., "Statistical properties of the periodic Lorentz gas. multidimensional case," *J. Stat. Phys.*, vol. 74, no. 1-2, pp. 11–53, 1994.

[22] Christ, N. H., Friedberg, R., and Lee, T. D., "Random lattice field theory: General formulation," *Nucl. Phys. B*, vol. 202, pp. 89–125, 1982.

[23] Cohen, E. G. D., "New types of diffusion in lattice gas cellular automata," in *Microscopic Simulations of Complex Hydrodynamic Phenomena* (Mareschal, M. and Holian, B. L., eds.), pp. 137–152, Plenum Press: New York, 1992.

[24] Cohen, E. G. D. and Wang, F., "New results for diffusion in Lorentz lattice gas cellular automata," *J. Stat. Phys.*, vol. 81, pp. 445–466, 1995. Also available at http://arxiv.org/comp-gas/9501003.

[25] Cohen, E. G. D. and Wang, F., "Novel phenomena in Lorentz lattice gas cellular automata," *Physica A*, vol. 219, pp. 56–87, 1995.

[26] Cohen, E. G. D. and Wang, F., *Diffusion and propagation in Lorentz lattice gases*, vol. 6 of *Fields Inst. Commun.*, pp. 43–54. Amer. Math. Soc., 1996.

[27] Dewdney, A. K., "Two-dimensional Turing machines and Turmites make tracks on a plane," *Scientific American*, vol. 261, pp. 180–183, September 1989.

[28] Dhar, A. and Dhar, D., "Absence of local thermal equilibrium in two models of heat conduction," *Phys. Rev. Lett.*, vol. 82, no. 3, pp. 480–483, 1999.

[29] Duplantier, B., "Hull percolation and standard percolation," *J. Phys. A*, vol. 21, pp. 3969–3973, 1988.

[30] Ehrenfest, P., *Collected Scientific Papers*. North-Holland: Amsterdam, 1959.

[31] Ernst, M. H. and van Velzen, G. A., "Lattice Lorentz gas," *J. Phys. A*, vol. 22, pp. 4611–4632, 1989.

[32] Ernst, M. H. and van Velzen, G. A., "Long-time tails in lattice Lorentz gases," *J. Stat. Phys.*, vol. 57, no. 3-4, pp. 455–471, 1989.

[33] Feller, W., *An Introduction to Probability Theory and Its Application*. Wiley: New York, second ed., 1971.

[34] Friedberg, R. and Ren, H.-C., "Field theory on a computationally constructed random lattice," *Nucl. Phys. B*, vol. 235[FS11], pp. 310–320, 1984.

[35] Frisch, U., Hasslacher, B., and Y.Pomeau, "Lattice-gas automata for the Navier-Stokes equation," *Phys. Rev. Lett.*, vol. 56, no. 14, pp. 1505–1508, 1986.

[36] Gajardo, A. and Mazoyer, J., "Langton's ant evolution in the degree 3 graphs," *Preprint*, 1999.

[37] Gajardo, A., Moreira, A., and Goles, E., "Complexity of Langton's ant," *Discr. App. Math.*, vol. 117, pp. 41–50, 2002.

[38] Green, P. J. and Sibson, R., "Computing Dirichlet tesselations in the plane," *Comp. J.*, vol. 21, no. 2, pp. 168–173, 1977.

[39] Grimmett, G. R., *Percolation*. Springer-Verlag: Berlin, 1989.

[40] Grimmett, G. R., Menshikov, M. V., and Volkov, S. E., "Random walks in random labyrinths," *Markov Proc. Rel. Fields*, vol. 2, no. 1, pp. 69–86, 1996. Disordered systems and statistical physics: Rigorous results (Budapest, 1995).

[41] Grosfils, P., Boon, J. P., Cohen, E. G. D., and Bunimovich, L. A., "Propagation and self-organization in lattice random media," *J. Stat. Phys.*, vol. 97, pp. 575–608, 1999. Also available at http://arxiv.org/cond-mat/9905168.

[42] Gunn, J. M. F. and M. Ortuño, "Percolation and motion in a simple random environment," *J. Phys. A*, vol. 18, pp. 1095–1099, 1985.

[43] Khlabystova, M., "One-dimensional many-particle Lorentz lattice gases: Statistical properties," *J. Stat. Phys*, submitted.

[44] Kong, X. P. and Cohen, E. G. D., "Anomalous diffusion in a lattice-gas wind-tree model," *Phys. Rev. B*, vol. 40, pp. 4838–4845, 1989.

[45] Kong, X. P. and Cohen, E. G. D., "Diffusion and propagation in triangular Lorentz lattice gas cellular automata," *J. Stat. Phys*, vol. 62, no. 3-4, pp. 737–757, 1991.

[46] Kong, X. P. and Cohen, E. G. D., "A kinetic theorist's look at lattice gas cellular automata," *Physica D*, vol. 47, pp. 9–18, 1991.

[47] Langton, C. G., "Studying artificial life with cellular automata," *Physica D*, vol. 22, pp. 120–149, 1986.

[48] Lorentz, H. A., "The motion of electrons in metallic bodies, I, II and III," *Koninklijke Akademie van Wetenschappen te Amsterdam, Section of Sciences*, vol. 7, pp. 438–453, 585–593, 684–691, 1905.

[49] Manna, S. and Guttmann, A., "Kinetic growth walks and trails on oriented square lattices: Hull percolation and percolation hulls," *J. Phys. A*, vol. 22, pp. 3113–3122, 1989.

[50] Mejía-Monasterio, C., Larralde, H., and Leyvraz, F., "Coupled normal heat and matter transport in a simple model system," *Phys. Rev. Lett.*, vol. 86, pp. 5417–5420, June 2001.

[51] Meng, H.-F. and Cohen, E. G. D., "Growth, self-randomization, and propagation in a lorentz lattice gas," *Phys. Rev. E*, vol. 50, no. 4, pp. 2482–2487, 1994.

[52] Moukarzel, C. and Herrmann, H. J., "A vectorizable random lattice," *J. Stat. Phys*, vol. 68, pp. 911–923, 1992.

[53] Okabe, A., Boots, B., and Sugihara, K., *Spatial tessellations: Concepts and applications of Voronoi diagrams*. Wiley: New York, 1992.

[54] Pickover, C., "Picturing randomness with Truchet tiles," *J. Recr. Math*, vol. 21, pp. 256–259, 1989.

[55] Pickover, C., "Mathematics and beauty: Several short classroom experiments," *AMS Notices*, vol. 38, no. 3, pp. 192–196, 1991.

[56] Rothman, D. H. and Zaleski, S., *Lattice-gas automata: Simple models of complex hydrodynamics*. Cambridge University Press, 1997.

[57] Roux, S., Guyon, E., and Sornette, D., "Hull percolation," *J. Phys. A*, vol. 21, pp. L475–L482, 1988.

[58] Ruijgrok, T. W. and Cohen, E. G. D., "Deterministic lattice gas models," *Phys. Lett. A*, vol. 133, pp. 415–418, 1988.

[59] Smith, C. S., "The tiling patterns of Sebastian Truchet and the topology of structural hierarchy," *Leonardo*, vol. 20, no. 4, pp. 373–385, 1987.

[60] van Velzen, G. A., *Lorentz lattice gases*. PhD thesis, University of Utrecht, 1990.

[61] Wang, F., *Motion in Lorentz lattice gases*. PhD thesis, The Rockefeller University, 1995.

[62] Wang, F. and Cohen, E. G. D., "Diffusion in Lorentz lattice gas cellular automata: The honeycomb and quasi-lattices compared with the square and triangular lattices," *J. Stat. Phys.*, vol. 81, pp. 467–475, 1995. Also available at http://arxiv.org/comp-gas/9501006.

[63] Wang, F. and Cohen, E. G. D., "Diffusion on random lattices," *J. Stat. Phys.*, vol. 84, pp. 233–261, 1996.

[64] Wolfram, S., "Cellular automaton fluids. I. basic theory," *J. Stat. Phys.*, vol. 45, no. 3-4, pp. 471–526, 1986. Also available at http://www.stephenwolfram.com/publications/articles/physics/86-fluids/index.html.

[65] Ziff, R. M., Kong, X. P., and Cohen, E. G. D., "Lorentz lattice-gas and kinetic-walk model," *Phys. Rev. A*, vol. 44, no. 4, pp. 2410–2428, 1991.

VITA

Milena Khlabystova was born in Saratov, Russia on December 6, 1972. In 1989 she graduated from a specialized high school with emphasis in mathematics and physics. Following her parents' footsteps, she decided to study geophysics and, in September, was admitted into the Faculty of Physics at St. Petersburg State University, Russia. A year and a half later, however, she encountered two fascinating persons who introduced her to the world of mathematics and became a constant source of inspiration. Thus, after achieving her Bachelor of Science degree in Physics with specialization in computational physics from St. Petersburg State University in 1994, she entered the Master of Science program in Theoretical and Mathematical Physics at the same University. In this program, she worked with her mentors, Drs. Ludmila Dmitrieva and Yuri Kuperin in the fields of spectral theory of operators and soliton solutions of partial differential equations, and co-authored three papers with Dr. Dmitrieva. In 1997, she graduated with honors and was accepted into the Ph. D. program in Mathematics at the Georgia Institute of Technology. Here she worked with Dr. Leonid Bunimovich, with whom she published four papers in the field of Lorentz lattice gases, in pursuit of her doctoral degree. She successfully defended her thesis entitled Dynamical and Statistical Properties of Lorentz Lattice Gases in April, 2003.

Dynamical and Statistical Properties of Lorentz Lattice Gases

Milena Khlabystova

98 pages

Directed by Dr. Leonid Bunimovich

The motion of a single particle or an ensemble of particles in Lorentz lattice gases was studied analytically and numerically. The simplest exact solutions were obtained for the recently introduced model of Lorentz gas with rotating scatterers. In some cases, the dynamics of a single particle in this model was shown to be identical to the dynamics in the one-dimensional model with flipping scatterers.

Kinetic equations and their continuous limits were obtained for the one-dimensional walks in rigid environments for all values of the rigidity. Due to the deterministic character of the dynamics, the obtained equations were of the Euler type. The effect of dependence between the scatterers at different lattice vertices was discussed.

Two-dimensional Lorentz gases with flipping rotators were studied on regular and random lattices. It was shown that for any distribution of scatterers in the flipping rotator model on the Delaunay random lattice the particle ultimately propagates in a strip, as it does on the regular triangular lattice; whereas such propagation does not occur on the regular square or hexagonal lattices. The probability of closed orbits on the Delaunay lattice was shown to be positive. For a certain general class of random lattices the motion of the particle was proven to be periodic with probabilty one.

In addition, computer simulations were performed for the one-dimensional multi-particle model with flipping scatterers. The observed distribution of the particle displacements appeared to be Gaussian at any time. In the fully occupied multi-particle model the motion of the particles was shown to be periodic with probability one.